

Analysis of $K_L \rightarrow \pi^+ \pi^- \gamma$ in Chiral Perturbation Theory *

GIANCARLO D'AMBROSIO[†] and JORGE PORTOLÉS[‡]

Istituto Nazionale di Fisica Nucleare, Sezione di Napoli
Dipartimento di Scienze Fisiche, Università di Napoli
I-80125 Napoli, Italy

Abstract

We study the long-distance dominated $K_L \rightarrow \pi^+ \pi^- \gamma$ decay at $\mathcal{O}(p^6)$ in Chiral Perturbation Theory. The complete calculation of the $\mathcal{O}(p^6)$ loop magnetic amplitude is carried out. At this chiral order the model dependent part of the vector meson exchange contribution to the magnetic amplitude is evaluated in the two models : FM (Factorization Model) and FMV (Factorization Model in the Vector Couplings). We predict, in an almost model independent way, a slope of $K_L \rightarrow \pi^+ \pi^- \gamma$ in the range $c \simeq -1.6, -1.8$, consistently with the experimental value. We find that the experimental result for the width of $K_L \rightarrow \pi^+ \pi^- \gamma$ is compatible with a bigger breaking of the nonet symmetry in the weak vertices than previously stated. Thus we conclude that our analysis does not exclude an opposite sign to the one given by the dominance of the pion pole in the poorly known $K_L \rightarrow \gamma \gamma$ amplitude. A complete analysis of the $\mathcal{O}(p^3)$ weak Vector-Pseudoscalar-Pseudoscalar (VPP) vertex is also performed.

PACS : 12.15.-y, 12.39.Fe, 12.40.Vv, 13.25.Es

Keywords : Radiative non-leptonic kaon decays, Non-leptonic weak hamiltonian, Chiral Perturbation Theory, Vector meson dominance.

[†] E-mail : dambrosio@axpna1.na.infn.it

[‡] E-mail : portoles@axpna1.na.infn.it

* Work supported in part by HCM, EEC-Contract No. CHRX-CT920026 (EURODAΦNE).

1 Introduction

Radiative non-leptonic kaon decays provide relevant tests for the ability of Chiral Perturbation Theory (χ PT) [1, 2] to explain weak low-energy processes. χ PT is a natural framework that embodies together an effective theory, satisfying the basic chiral symmetry of QCD, and a perturbative expansion in masses and external momenta that becomes the practical tool to work with. Its success in the study of radiative non-leptonic kaon decays has been remarkable (see Refs. [3, 4] and references therein).

Moreover the chiral anomaly present in the Standard Model manifests mainly in the low-energy interactions of the pseudoscalar mesons, and consequently χ PT is the appropriate framework to study those effects. As has already been shown [5, 6], radiative kaon decays are sensitive to the chiral anomaly in the non-leptonic sector. The study of these decays driven by the chiral anomaly ($K \rightarrow \pi\pi\gamma$, $K \rightarrow \pi\pi\gamma\gamma$, etc.) has thoroughly been carried out previously in the Refs. [5, 6, 7, 8] where their relevant features have been discussed.

The main uncertainty still present in the computation of those channels is the contribution from local terms that, in principle, appear at any order in the chiral expansion. At $\mathcal{O}(p^4)$ vector meson exchange (when present) has been shown to be effective in predicting the relevant couplings in the strong sector [9, 10]. However our poor phenomenological knowledge of the weak processes involving meson resonances translates into our ignorance about the couplings in weak counterterms at $\mathcal{O}(p^4)$ and beyond, thus models are required. In particular the Factorization Model (FM) [11] has been widely employed in this task [12, 13]. In Ref. [14] we proposed an implementation of the FM in the Vector Couplings (FMV) as a more efficient way of including the contributions of vector mesons into the weak couplings at $\mathcal{O}(p^6)$ in the processes $K \rightarrow \pi\gamma\gamma$ and $K_L \rightarrow \gamma\ell^+\ell^-$. We reached a good phenomenological description of both channels and showed that with the new vector contributions included no enhancement due to $\Delta I = 1/2$ transitions is required, in opposition to previous statements in the FM.

The basic statement of the FMV is to use the idea of factorization in order to construct the weak vertices involving vector mesons instead of implementing factorization in the strong lagrangian generated by vector exchange once the vector degrees of freedom have already been integrated out. The apparently tiny difference between both realizations has proven to be crucial in disentangling the rôle of the FM in uncovering new chiral structures that were absent in the standard approach and consequently giving a deeper understanding of the underlying physics.

In the present article we present the application of these ideas to the process $K_L \rightarrow \pi^+\pi^-\gamma$. This decay brings new features to our previous work. While in $K \rightarrow \pi\gamma\gamma$ and $K_L \rightarrow \gamma\ell^+\ell^-$ only the weak $\mathcal{O}(p^3)$ Vector-Pseudoscalar-Photon ($VP\gamma$) vertex is involved, now in $K_L \rightarrow \pi^+\pi^-\gamma$ we also need to consider the weak $\mathcal{O}(p^3)$ Vector-Pseudoscalar-Pseudoscalar (VPP) vertex. The interest in studying this particular process has a twofold purpose: a) the relevance of the process by itself given the fact that phenomenologically

constitutes an appropriate target of χ PT , and b) the dependence of this channel in the breaking of nonet symmetry in the weak sector. Let us comment these two aspects in turn.

As studied time ago [15] the process $K_L \rightarrow \pi^+\pi^-\gamma$ is driven by long–distance contributions. The Direct Emission amplitude of the decay is dominated by a magnetic type amplitude which slope in the photon energy in the kaon rest frame (to be defined properly in Section 4) has been measured experimentally. Even when the error is still a rough 30 % the slope seems rather big, a feature to be explained in χ PT as a contribution starting at $\mathcal{O}(p^6)$. Hence this fact together with our poor knowledge of the constant amplitude deserves a careful treatment. At $\mathcal{O}(p^6)$ chiral loops are present too, thus we have also performed the full loop evaluation at this chiral order. It turns out to be relevant for the stability of our slope prediction.

In Ref. [14] we pointed out that the experimental slope of $K_L \rightarrow \gamma\gamma^*$ and the theoretical vector meson dominance prediction cannot be accommodated unless the $K_L \rightarrow \gamma\gamma$ amplitude departs drastically (change sign) from the one predicted by the nonet symmetry. We would like to suggest that at the origin of this problem could be a large breaking of the nonet symmetry in the weak vertex. A way to explore this possibility is to study this hypothesis in another process sensitive to this breaking: $K_L \rightarrow \pi^+\pi^-\gamma$ receives an $\mathcal{O}(p^6)$ contribution due to anomalous reducible amplitudes [5, 7] where the nonet breaking plays a major rôle. Therefore we would like to investigate also the possibility of a satisfactory simultaneous description of the processes $K_L \rightarrow \gamma\gamma$ and $K_L \rightarrow \pi^+\pi^-\gamma$.

In Section 2 we will remind briefly the basic features of χ PT and its application to weak processes. Then in Section 3 we will specify the general characteristics and notation for $K_L \rightarrow \pi^+\pi^-\gamma$ and we will offer a short overview of the process in χ PT . The $\mathcal{O}(p^6)$ contributions to the magnetic amplitude will be collected and explained in Section 4. The analysis of the combined observables will be carried out in Section 5 while we will emphasize our conclusions in Section 6. Three brief appendices complement the main text.

2 Non-leptonic weak interactions at low energies

We will review in this Section the procedures of χ PT and their implementation in the study of non-leptonic weak processes. We will collect also the tools we will need in the development of our study.

2.1 Chiral Perturbation Theory

χ PT [1, 2] is an effective quantum field theory for the study of low energy strong interacting processes that relies in the exact global chiral symmetry of massless QCD.

The basic assumption is that, at low energies ($E \leq 1 \text{ GeV}$), the chiral symmetry group $G \equiv SU(3)_L \otimes SU(3)_R$ is spontaneously broken to the vector subgroup $SU(3)_V$, generating eight Goldstone bosons to be identified with the lightest octet of pseudoscalar mesons (φ_i). These are conveniently parameterized by a $SU(3)$ matrix field

$$U(\varphi) = \exp \left(\frac{i}{F} \sum_{j=1}^8 \lambda_j \varphi_j \right) , \quad (1)$$

that transforms linearly under the chiral group G . In Eq. (1) λ_i are the $SU(3)$ Gell–Mann matrices ¹ and $F \sim F_\pi \simeq 93 \text{ MeV}$ is the decay constant of the pion.

The extension of the global chiral symmetry to a local one and the inclusion of external fields are convenient tools in order to work out systematically the Green functions of interest and the construction of chiral operators in the presence of symmetry breaking terms. A covariant derivative on the U field is then defined as

$$D_\mu U = \partial_\mu U - ir_\mu U + iU\ell_\mu , \quad (2)$$

where $\ell_\mu = v_\mu - a_\mu$ and $r_\mu = v_\mu + a_\mu$, are the left and right external fields, respectively, in terms of the external vector and axial–vector fields. If only the electromagnetic field is considered then $\ell_\mu = r_\mu = -eQA_\mu$ where $Q \equiv \text{diag}(2/3, -1/3, -1/3)$ is the electric charge matrix of the u , d and s quarks ². The explicit breaking of the chiral symmetry due to the masses of the octet of pseudoscalars is included through the external scalar field $s = \mathcal{M} + \dots$. In this way an effective lagrangian can be constructed as an expansion in the external momenta (derivatives of the Goldstone fields) and masses [1, 2, 16].

The leading $\mathcal{O}(p^2)$ strong lagrangian is

$$\mathcal{L}_2 = \frac{F^2}{4} \langle u_\mu u^\mu + \chi_+ \rangle , \quad (3)$$

where $\langle A \rangle \equiv \text{Tr}(A)$ in the flavour space and

$$\begin{aligned} u_\mu &= i u^\dagger D_\mu U u^\dagger & , & & U &= u^2 & , \\ \chi_+ &= u^\dagger \chi u^\dagger + u \chi^\dagger u & , & & \chi &= 2 B_\circ (s + ip) = 2 B_\circ \mathcal{M} + \dots & , \\ \mathcal{M} &= \text{diag}(m_u, m_d, m_s) & , & & B_\circ &= -\frac{1}{F^2} \langle 0 | \bar{u}u | 0 \rangle . \end{aligned} \quad (4)$$

The even-intrinsic parity lagrangian at $\mathcal{O}(p^4)$ was developed in Ref. [2] and introduces 12 new coupling constants. For our work the only piece we will need is

$$\mathcal{L}_4 = -i L_9 \langle f_+^{\mu\nu} u_\mu u_\nu \rangle + \dots , \quad (5)$$

where

$$f_\pm^{\mu\nu} = u F_L^{\mu\nu} u^\dagger \pm u^\dagger F_R^{\mu\nu} u , \quad (6)$$

¹ Normalized to $\text{Tr}(\lambda_i \lambda_j) = 2\delta_{ij}$.

²This corresponds to $D_\mu \phi^\pm = (\partial_\mu \pm ieA_\mu)\phi^\pm$.

and $F_{R,L}^{\mu\nu}$ are the strength field tensors associated to the external r_μ and ℓ_μ fields, respectively. From the experimental value of the pion charge radius one obtains $L_9^r(m_\rho) = (6.9 \pm 0.7) \times 10^{-3}$.

The $\mathcal{O}(p^4)$ odd-intrinsic parity lagrangian arises as a solution to the Ward condition imposed by the chiral anomaly [17]. The chiral anomalous functional $Z_{an}[U, \ell, r]$ as given by the Wess-Zumino-Witten action (WZW) is

$$\begin{aligned} Z_{an}[U, \ell, r]_{WZW} &= -\frac{iN_c}{240\pi^2} \int_{M^5} d^5x \epsilon^{ijklm} \langle \Sigma_i^L \Sigma_j^L \Sigma_k^L \Sigma_l^L \Sigma_m^L \rangle \\ &\quad - \frac{iN_c}{48\pi^2} \int d^4x \epsilon_{\mu\nu\alpha\beta} (W(U, \ell, r)^{\mu\nu\alpha\beta} - W(I, \ell, r)^{\mu\nu\alpha\beta}), \end{aligned} \quad (7)$$

$$\begin{aligned} W(U, \ell, r)_{\mu\nu\alpha\beta} &= \langle U \ell_\mu \ell_\nu \ell_\alpha U^\dagger r_\beta + \frac{1}{4} U \ell_\mu U^\dagger r_\nu U \ell_\alpha U^\dagger r_\beta + i U \partial_\mu \ell_\nu \ell_\alpha U^\dagger r_\beta \\ &\quad + i \partial_\mu r_\nu U \ell_\alpha U^\dagger r_\beta - i \Sigma_\mu^L \ell_\nu U^\dagger r_\alpha U \ell_\beta + \Sigma_\mu^L U^\dagger \partial_\nu r_\alpha U \ell_\beta \\ &\quad - \Sigma_\mu^L \Sigma_\nu^L U^\dagger r_\alpha U \ell_\beta + \Sigma_\mu^L \ell_\nu \partial_\alpha \ell_\beta + \Sigma_\mu^L \partial_\nu \ell_\alpha \ell_\beta \\ &\quad - i \Sigma_\mu^L \ell_\nu \ell_\alpha \ell_\beta + \frac{1}{2} \Sigma_\mu^L \ell_\nu \Sigma_\alpha^L \ell_\beta - i \Sigma_\mu^L \Sigma_\nu^L \Sigma_\alpha^L \ell_\beta \rangle \\ &\quad - (L \leftrightarrow R), \end{aligned} \quad (8)$$

with $N_c = 3$, $\Sigma_\mu^L = U^\dagger \partial_\mu U$, $\Sigma_\mu^R = U \partial_\mu U^\dagger$ and $(L \leftrightarrow R)$ stands for the interchange $U \leftrightarrow U^\dagger$, $\ell_\mu \leftrightarrow r_\mu$, $\Sigma_\mu^L \leftrightarrow \Sigma_\mu^R$. We notice that the WZW action does not include any unknown coupling.

The inclusion of other quantum fields than the pseudoscalar Goldstone bosons in the chiral lagrangian was considered in Ref. [18]. We are interested in the introduction of vector mesons coupled to the $U(\varphi)$ and to the external fields. Let us then introduce the nonet of vector fields

$$V_\mu = \frac{1}{\sqrt{2}} \sum_{i=1}^8 \lambda_i V_\mu^i + \frac{1}{\sqrt{3}} V_\mu^0, \quad (9)$$

that transforms homogeneously under the chiral group G . Here ideal mixing, i.e. $V_\mu^8 = (\omega_\mu + \sqrt{2}\phi_\mu)/\sqrt{3}$, is assumed.

The most general strong and electromagnetic lagrangian, at leading $\mathcal{O}(p^3)$ and assuming nonet symmetry, with the vector field linearly coupled to the Goldstone bosons, is given by the following terms [19]

$$\begin{aligned} \mathcal{L}_V &= -\frac{f_V}{2\sqrt{2}} \langle V_{\mu\nu} f_+^{\mu\nu} \rangle - i \frac{g_V}{2\sqrt{2}} \langle V_{\mu\nu} [u^\mu, u^\nu] \rangle + h_V \epsilon_{\mu\nu\rho\sigma} \langle V^\mu \{u^\nu, f_+^{\rho\sigma}\} \rangle \\ &\quad + i \theta_V \epsilon_{\mu\nu\rho\sigma} \langle V^\mu u^\nu u^\rho u^\sigma \rangle, \end{aligned} \quad (10)$$

where only the relevant pieces for our work have been written. In Eq. (10) $V_{\mu\nu} = \nabla_\mu V_\nu - \nabla_\nu V_\mu$ and ∇_μ is the covariant derivative defined in Ref. [9] as

$$\nabla_\mu V_\nu = \partial_\mu V_\nu + [\Gamma_\mu, V_\nu] , \tag{11}$$

$$\Gamma_\mu = \frac{1}{2} \left\{ u^\dagger (\partial_\mu - ir_\mu) u + u (\partial_\mu - il_\mu) u^\dagger \right\} .$$

The couplings in Eq. (10) can be determined phenomenologically from the experiment [20]. The experimental width $\Gamma(\omega \rightarrow \pi^0 \gamma)$ gives $|h_V| \simeq 0.037$ [21]. Also from $\Gamma(\rho^0 \rightarrow e^+ e^-)$ one gets $|f_V| \simeq 0.20$ and from $\Gamma(\rho^0 \rightarrow \pi^+ \pi^-)$ $|g_V| \simeq 0.09$ [9]. Moreover the positive slope of the $\pi^0 \rightarrow \gamma \gamma^*$ form factor determined experimentally imposes $h_V f_V > 0$. The resonance saturation of the $\mathcal{O}(p^4)$ couplings gives [9] $L_9 = f_V g_V / 2$ in Eq. (5) and the positivity, determined phenomenologically, of $L_9^r(m_\rho)$ implies $f_V g_V > 0$. In the Hidden Gauge Model [22] the relations $f_V = 2g_V$ and $\theta_V = 2h_V$ arise. The first one is in excellent agreement with the experimental determination while the second is in good agreement with the ENJL model results [23]. We will assume them throughout the paper.

The introduction of the axial-vector nonet defined analogously to the vector in Eq. (9) is similar to the latter. The interaction terms we will need are

$$\mathcal{L}_A = -\frac{f_A}{2\sqrt{2}} \langle A_{\mu\nu} f^{\mu\nu} \rangle + h_A \varepsilon_{\mu\nu\alpha\beta} \langle A^\mu \{u^\nu, f^{\alpha\beta}\} \rangle , \tag{12}$$

with $A_{\mu\nu}$ defined as in the vector case above. The couplings f_A and h_A could be determined from radiative decays. Due to the poor phenomenology available on axial-vector decays we rely on theoretical predictions [19, 23] that give $f_A \simeq 0.09$ and $h_A \simeq 0.014$.

The incorporation of spin-1 mesons in chiral lagrangians is not unique and several realizations of the vector field can be employed [24]. In Ref. [19] was proven that at $\mathcal{O}(p^4)$ in χ PT and once high energy QCD constraints are taken into account, the usual realizations (antisymmetric tensor, vector field, Yang-Mills and Hidden formulations) are equivalent. Although the antisymmetric tensor formulation of spin-1 mesons was proven to have a better high-energy behaviour than the vector field realization at $\mathcal{O}(p^4)$, this fact is not necessarily the case in general. In fact for the odd-intrinsic parity operator relevant in the $V \rightarrow P\gamma$ decay, the antisymmetric tensor formulation would give contributions starting at $\mathcal{O}(p^4)$ while QCD requires an explicit $\mathcal{O}(p^3)$ term as given by the vector realization in the h_V term in Eq. (10) [21]³. Moreover we have pointed out that the conventional vector formulation seems to give a complete and consistent treatment of the spin-1 resonance generated weak couplings at $\mathcal{O}(p^4)$ [26] and $\mathcal{O}(p^6)$ [14].

For a further extensive and thorough exposition on χ PT see Ref. [27].

³For a more detailed discussion of the equivalence of vector resonance models in the odd-intrinsic parity violating sector see Ref. [25].

2.2 Non-leptonic weak interactions in χ PT

At low energies ($E \ll M_W$) the $\Delta S = 1$ effective hamiltonian is obtained from the Lagrangian of the Standard Model by using the asymptotic freedom property of QCD in order to integrate out the fields with heavy masses down to scales $\mu < m_c$. It reads [28]

$$\mathcal{H}_{NL}^{|\Delta S|=1} = -\frac{G_F}{\sqrt{2}} V_{ud} V_{us}^* \sum_{i=1}^6 C_i(\mu) Q_i + h.c. . \quad (13)$$

Here G_F is the Fermi constant, V_{ij} are elements of the CKM matrix and $C_i(\mu)$ are the Wilson coefficients of the four-quark operators Q_i , $i = 1, \dots, 6$.

At $\mathcal{O}(p^2)$ in χ PT we can construct only one relevant octet effective operator using the left-handed currents associated to the chiral transformations,

$$\begin{aligned} \mathcal{L}_2^{|\Delta S|=1} &= 4 \frac{G_F}{\sqrt{2}} V_{ud} V_{us}^* g_8 \langle \lambda_6 L_1^\mu L_\mu^1 \rangle \\ &= \frac{G_F}{\sqrt{2}} F^4 V_{ud} V_{us}^* g_8 \langle \Delta u_\mu u^\mu \rangle , \end{aligned} \quad (14)$$

where

$$L_\mu^1 = \frac{\delta S_2^X}{\delta \ell^\mu} = -i \frac{F^2}{2} U^\dagger D_\mu U = -\frac{F^2}{2} u^\dagger u_\mu u , \quad (15)$$

is the left-handed current associated to the S_2^X action of the $\mathcal{O}(p^2)$ strong lagrangian in Eq. (3), $\Delta = u \lambda_6 u^\dagger$ and g_8 is an effective coupling.

From the experimental width of $K \rightarrow \pi\pi$ one gets at $\mathcal{O}(p^2)$

$$|g_8|_{K \rightarrow \pi\pi} \simeq 5.1 \quad , \quad G_8 \equiv \frac{G_F}{\sqrt{2}} V_{ud} V_{us}^* |g_8|_{K \rightarrow \pi\pi} \simeq 9.2 \times 10^{-6} \text{ GeV}^{-2} . \quad (16)$$

In our analysis of $K_L \rightarrow \pi^+ \pi^- \gamma$ the singlet pseudoscalar η_0 contributes at $\mathcal{O}(p^6)$. If nonet symmetry is broken weak interactions of the singlet at $\mathcal{O}(p^2)$ have to be parameterized through a new coupling : ρ . Then

$$\mathcal{L}_{\eta'}^{|\Delta S|=1} = \frac{2}{3} G_8 F^4 (\rho - 1) \langle \Delta u_\mu \rangle \langle u^\mu \rangle , \quad (17)$$

should be added to $\mathcal{L}_2^{|\Delta S|=1}$ in Eq. (14).

At $\mathcal{O}(p^4)$ the weak chiral lagrangian has been studied in Refs. [12, 29, 30] giving 37 chiral operators only in the octet part. For the study of anomalous radiative decays only four of them are relevant,

$$\begin{aligned} \mathcal{L}_4^{|\Delta S|=1} &= G_8 F^2 \varepsilon_{\mu\nu\alpha\beta} \left[i N_{28} \langle \Delta u^\mu \rangle \langle u^\nu u^\alpha u^\beta \rangle + N_{29} \langle \Delta [f_+^{\alpha\beta} - f_-^{\alpha\beta}] , u^\mu u^\nu \rangle \right. \\ &\quad \left. + N_{30} \langle \Delta u^\mu \rangle \langle f_+^{\alpha\beta} u^\nu \rangle + N_{31} \langle \Delta u^\mu \rangle \langle f_-^{\alpha\beta} u^\nu \rangle \right] + \dots , \end{aligned} \quad (18)$$

where N_{28}, \dots, N_{31} are new coupling constants to be determined phenomenologically or predicted by models.

Motivated by $1/N_c$ arguments the concept of factorization has been developed in the context of χ PT . In the $N_c \rightarrow \infty$ limit penguin operators are suppressed. Then if the effect of gluon exchange at leading order is considered and we assume octet dominance through current–current operators in Eq. (13) we have [28]

$$\mathcal{H}_{NL}^{|\Delta S|=1} = -\frac{G_F}{2\sqrt{2}} V_{ud}V_{us}^* C_-(\mu) Q_- + h.c. , \quad (19)$$

where

$$Q_- = 4(\bar{s}_L\gamma^\mu u_L)(\bar{u}_L\gamma_\mu d_L) - 4(\bar{s}_L\gamma^\mu d_L)(\bar{u}_L\gamma_\mu u_L) , \quad (20)$$

with $\bar{q}_{1L}\gamma_\mu q_{2L} \equiv \frac{1}{2}\bar{q}_1^\alpha\gamma_\mu(1-\gamma_5)q_{2\alpha}$ and α a colour index. The Q_- operator transforms under $SU(3)_L \otimes SU(3)_R$ as the $(8_L, 1_R)$ representation. The result for the Wilson coefficient $C_-(m_\rho)$ at leading $\mathcal{O}(\alpha_s)$ and with $\Lambda_{\overline{MS}} = 325$ MeV is

$$C_-(m_\rho) \simeq 2.2 \quad \longrightarrow \quad g_8 \simeq 1.1 , \quad (21)$$

to be compared with Eq. (16). In a chiral gauge theory the quark bilinears in the Q_- operator in Eq. (20) are given by the associated left–handed current

$$\frac{\delta S}{\delta \ell^\mu} = L_\mu^1 + L_\mu^3 + L_\mu^5 + \dots , \quad (22)$$

(the first term L_μ^1 was already given in Eq. (15)) where $S[U, \ell, r, s, p]$ is the low–energy strong effective action of QCD in terms of the Goldstone bosons realization U and the external fields ℓ, r, s, p . The assumption of Factorization amounts to write the four–quark operators in the factorized *current* \times *current* form as

$$\mathcal{L}_{FM} = 4k_F G_8 \langle \lambda \frac{\delta S}{\delta \ell_\mu} \frac{\delta S}{\delta \ell^\mu} \rangle + h.c. , \quad (23)$$

where $\lambda \equiv \frac{1}{2}(\lambda_6 - i\lambda_7)$ and k_F is an overall factor not given by the model. In general $k_F \simeq \mathcal{O}(1)$ and naive factorization would imply $k_F \simeq 1$. However the Wilson coefficient of the Q_- operator would give $k_F \simeq 0.2 - 0.3$ as follows from Eq. (21).

It has become customary in the literature [6, 7] to introduce the a_i couplings defined through

$$\begin{aligned} N_{28} &= \frac{a_1}{8\pi^2} , & N_{29} &= \frac{a_2}{32\pi^2} , \\ N_{30} &= \frac{3a_3}{16\pi^2} , & N_{31} &= \frac{a_4}{16\pi^2} . \end{aligned} \quad (24)$$

In Refs. [6, 31] the FM was used to evaluate the factorizable contribution of the chiral anomaly (WZW action in Eq. (7)) to these couplings, giving $a_i^{an} = \eta_{an}$, $i = 1, 2, 3, 4$, with $\eta_{an} \sim \mathcal{O}(1)$ and positive the unknown FM factor. Non–factorizable contributions do not add any new chiral structure to these.

This same model predicts vanishing resonance contributions to these couplings if the antisymmetric formulation for the spin-1 fields is used. In Ref. [26] we have evaluated the spin-1 resonance contributions (vector and axial-vector) to the N_i couplings using a novel framework in which the vector formulation of the resonance fields is implemented. We quote here the relevant results for our case using factorization. These are

$$\begin{aligned}
N_{28}^{V+A} &= \sqrt{2} f_V \theta_V \eta_V , \\
N_{29}^{V+A} &= \frac{1}{\sqrt{2}} (f_V h_V \eta_V - f_A h_A \eta_A) , \\
N_{30}^{V+A} &= 2\sqrt{2} f_V h_V \eta_V , \\
N_{31}^{V+A} &= 2\sqrt{2} f_A h_A \eta_A ,
\end{aligned} \tag{25}$$

where f_V , h_V , θ_V , f_A and h_A have been defined in Eqs. (10,12), and η_V , η_A are the undetermined factorization parameters. We have, therefore, three unknown couplings : η_{an} , η_V and η_A . We remind that naive factorization, however, implies $\eta_{an} = \eta_V = \eta_A \equiv \eta$. Once we determine the N_i couplings from the phenomenology of $K_L \rightarrow \pi^+ \pi^- \gamma$ (see Section 5) for sake of definiteness we will assume the naive FM relation. In this way we reduce the four N_i couplings to only one free parameter.

3 The $K_L \rightarrow \pi^+ \pi^- \gamma$ amplitudes in χ PT

The general amplitude for $K \rightarrow \pi \pi \gamma$ is given by

$$A[K(p) \rightarrow \pi_1(p_1) \pi_2(p_2) \gamma(q, \epsilon)] = \epsilon^{\mu*}(q) M_\mu(q, p_1, p_2) , \tag{26}$$

where $\epsilon_\mu(q)$ is the photon polarization and M_μ is decomposed into an electric E and a magnetic M amplitudes as

$$M_\mu = \frac{E(z_i)}{m_K^3} [p_1 \cdot q p_{2\mu} - p_2 \cdot q p_{1\mu}] + \frac{M(z_i)}{m_K^3} \epsilon_{\mu\nu\rho\sigma} p_1^\nu p_2^\rho q^\sigma , \tag{27}$$

with

$$z_i = \frac{q \cdot p_i}{m_K^2} , (i = 1, 2) \quad , \quad z_3 = \frac{p \cdot q}{m_K^2} \quad , \quad z_3 = z_1 + z_2 . \tag{28}$$

The invariant amplitudes $E(z_i)$, $M(z_i)$ are dimensionless. Adding over photon helicities there is no interference between both amplitudes and the double differential rate for an unpolarized photon is given by

$$\frac{\partial^2 \Gamma}{\partial z_1 \partial z_2} = \frac{m_K}{(4\pi)^3} \left(|E(z_i)|^2 + |M(z_i)|^2 \right) \left[z_1 z_2 (1 - 2(z_1 + z_2) - r_1^2 - r_2^2) - r_1^2 z_2^2 - r_2^2 z_1^2 \right] , \tag{29}$$

where $r_i = m_{\pi_i}/m_K$. In Appendix A we recall, for completeness, some of the kinematical relations for $K_L \rightarrow \pi^+ \pi^- \gamma$.

The total amplitude of $K \rightarrow \pi\pi\gamma$ can be decomposed as a sum of *inner bremsstrahlung* (IB) and *direct emission* (DE) (or structure dependent) amplitudes. The electric amplitude $E_{IB}(z_i)$ arises already at $\mathcal{O}(p^2)$ in χ PT and it is completely predicted by the Low theorem [32] which relates radiative and non-radiative amplitudes in the limit of the photon energy going to zero. Due to the pole in the photon energy the IB amplitude generally dominates unless the non-radiative amplitude is suppressed due to some particular reason. This is the case of $K_L \rightarrow \pi^+\pi^-\gamma$ (where $K_2^0 \rightarrow \pi^+\pi^-$ is CP violating [7, 8]) or $K^+ \rightarrow \pi^+\pi^0\gamma$ (where $K^+ \rightarrow \pi^+\pi^0$ is suppressed by the $\Delta I = 1/2$ rule). These channels are important in order to extract the DE amplitude that reveals the chiral structure of the process. In this article we are going to focus our attention in the $K_L \rightarrow \pi^+\pi^-\gamma$ channel (for a thorough overview of other channels see Refs. [7, 8]).

DE contributions can be decomposed in a multipole expansion [33, 34]. In our following discussion we will consider only CP-conserving DE amplitudes. These start at $\mathcal{O}(p^4)$ in χ PT where E2 and M1 multipoles are generated. Due to the asymmetry under the interchange of pion momenta of the E2 amplitude there are no local contributions and then it is only generated by a finite chiral loop amplitude $E_{loop}^{(4)}$. It was computed in Refs. [5, 8]. The amplitude $E_{loop}^{(4)}$ gives an E2 multipole very suppressed in comparison with the IB, typically [7], $|E_{loop}^{(4)}/E_{IB}| \leq 10^{-2}$. This is due to several circumstances: chiral loop suppression, absence of the photon energy pole and asymmetry under the interchange of pion momenta. Higher order terms, though in principle could be larger, still generate very small interference with the IB amplitude [8]. Thus we will neglect here the electric amplitudes.

In fact the experimental results [35] for the branching ratio of $K_L \rightarrow \pi^+\pi^-\gamma$ are consistent with the IB ($Br(K_L \rightarrow \pi^+\pi^-\gamma; E_\gamma^* > 20 \text{ MeV})_{IB} = (1.49 \pm 0.08) \times 10^{-5}$), and a dipole magnetic contribution

$$Br(K_L \rightarrow \pi^+\pi^-\gamma; E_\gamma^* > 20 \text{ MeV})_{DE} = (3.19 \pm 0.16) \times 10^{-5}, \quad (30)$$

where E_γ^* is the photon energy in the kaon rest frame.

In opposition to the electric case the M1 multipole at leading $\mathcal{O}(p^4)$ is generated by a constant local contribution only. This is given by $\mathcal{L}_4^{|\Delta S|=1}$ in Eq. (18) through the diagram in Fig. 1.a and the result is

$$\begin{aligned} M^{(4)} &= -\frac{G_8 e m_K^3}{2\pi^2 F_\pi} [32\pi^2 (N_{29} + N_{31})] \\ &= -\frac{G_8 e m_K^3}{2\pi^2 F_\pi} (a_2 + 2a_4). \end{aligned} \quad (31)$$

As there is no loop contribution at this order the combination of couplings $N_{29} + N_{31}$ is scale independent ⁴. These couplings are unknown from the phenomenology and this

⁴In fact all the anomalous couplings in $\mathcal{L}_4^{|\Delta S|=1}$ in Eq. (18) are separately scale independent because there is no intrinsic parity violating action at $\mathcal{O}(p^2)$.

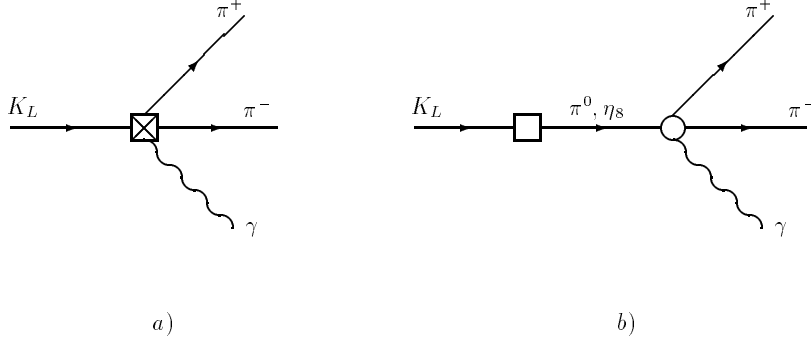


Figure 1: Diagrams contributing to the $\mathcal{O}(p^4)$ magnetic amplitude $M^{(4)}$. The diagram b) is vanishing at this order. The crossed box corresponds to a vertex generated by the $\mathcal{L}_4^{|\Delta S|=1}$ lagrangian in Eq. (18), the empty box is generated by $\mathcal{L}_2^{|\Delta S|=1}$ in Eq. (14) and the circle by the WZW action Z_{an} in Eq. (7).

fact constrains our knowledge on this contribution. At $\mathcal{O}(p^4)$ one could also consider the reducible anomalous magnetic amplitude generated by the diagram in Fig. 1.b. However at this chiral order this amplitude vanishes because the Gell-Mann–Okubo mass relation as happens in $K_L \rightarrow \gamma\gamma$. Due to this cancellation and the possibility that the combination $a_2 + 2a_4$ is small, the $\mathcal{O}(p^6)$ contributions seem theoretically important. Also the experimental analysis carried out in Ref. [35] shows a clear dependence in the photon energy that appears in the magnetic amplitude only at $\mathcal{O}(p^6)$. It is therefore necessary to study the $\mathcal{O}(p^6)$ contributions to the magnetic amplitude in order to be able to analyse thoroughly this decay. This we will do in the following Sections.

4 Magnetic amplitude of $K_L \rightarrow \pi^+\pi^-\gamma$ at $\mathcal{O}(p^6)$

Both local terms and chiral loops contribute to a magnetic amplitude for $K_L \rightarrow \pi^+\pi^-\gamma$ at $\mathcal{O}(p^6)$ in χ PT. As commented before the first dependence of the magnetic amplitude in the photon energy appears at this chiral order.

The magnetic amplitude can be expressed as

$$M = -\frac{G_8 e m_K^3}{2\pi^2 F_\pi} \tilde{m} (1 + c z_3), \quad (32)$$

where $|\widetilde{m}|$ and the slope c are fixed by the rate and the spectrum, respectively ⁵. From the experimental results ⁶ in Ref. [35] we have

$$|\widetilde{m}|_{exp} = 1.53 \pm 0.25 ,$$

$$c_{exp} = -1.7 \pm 0.5 ,$$
(33)

where the error in $|\widetilde{m}|_{exp}$ comes only from the error in the slope. z_3 has been defined in Eq. (28) and in the K_L rest frame $z_3 = E_\gamma^*/m_K$.

As can be noticed the dependence on the photon energy is by no means negligible. However we have seen that it is vanishing at $\mathcal{O}(p^4)$ in Eq. (31) and then it is a goal of the higher orders in χ PT to accommodate such a big value.

4.1 Local amplitudes

There are different local contributions to $K_L \rightarrow \pi^+\pi^-\gamma$ starting at $\mathcal{O}(p^6)$. Some of them are model independent while in some other cases one has to use models. Here we do an analysis of all of them at this chiral order.

First of all there is a reducible anomalous amplitude given by the diagram in Fig. 2. This is the same that the vanishing one in Fig. 1.b but now the π^0 , η and η' are included. Then it is $\mathcal{O}(p^6)$ (but also contains higher orders) and is given by

$$M_{anom}^{(6)} = \frac{G_8 e m_K^3}{2\pi^2 F_\pi} F_1 ,$$
(34)

where

$$F_1 = \frac{1}{1-r_\pi^2} + \frac{1}{3(1-r_\eta^2)} [(1+\xi)\cos\theta + 2\sqrt{2}\rho\sin\theta] \left[\left(\frac{F_\pi}{F_8}\right)^3 \cos\theta - \sqrt{2}\left(\frac{F_\pi}{F_0}\right)^3 \sin\theta \right] - \frac{1}{3(1-r_{\eta'}^2)} [2\sqrt{2}\rho\cos\theta - (1+\xi)\sin\theta] \left[\left(\frac{F_\pi}{F_8}\right)^3 \sin\theta + \sqrt{2}\left(\frac{F_\pi}{F_0}\right)^3 \cos\theta \right] .$$
(35)

In F_1 , $r_P \equiv m_P/m_K$, ξ parameterizes the $SU(3)$ breaking defined through

$$\frac{\langle \eta_8 | \mathcal{L}^{|\Delta S|=1} | K_2^0 \rangle}{\langle \pi^0 | \mathcal{L}^{|\Delta S|=1} | K_2^0 \rangle} = \frac{1}{\sqrt{3}} (1 + \xi) ,$$
(36)

θ denotes the η - η' mixing angle, ρ has been defined in Eq. (17) and F_8 , F_0 are the decay constants of η_8 and η_0 , respectively. At $\mathcal{O}(p^4)$ F_1 vanishes because the Gell-Mann–Okubo mass relation. We note that $M_{anom}^{(6)}$ is constant and has no dependence on the photon energy.

⁵Neglecting the Electric multipoles in the total DE amplitude.

⁶The value of the slope is given by E.J. Ramberg in private communication reported in Ref. [7]. The central value can also be followed from Ref. [35].

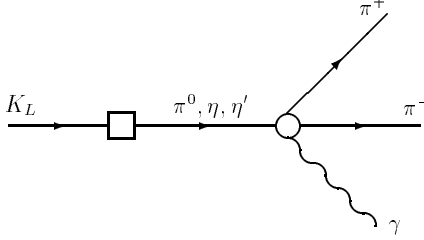


Figure 2: Diagram contributing to the reducible anomalous $\mathcal{O}(p^6)$ magnetic amplitude $M_{anom}^{(6)}$. The empty box is generated by $\mathcal{L}_2^{|\Delta S|=1} + \mathcal{L}_{\eta'}^{|\Delta S|=1}$ in Eqs. (14, 17) and the white circle by the WZW action Z_{an} in Eq. (7).

Other $\mathcal{O}(p^6)$ local amplitudes can be generated through resonance interchange. In particular we are going to focus in the vector meson contributions which are reasonably thought to be the most relevant ones. There are two different kinds of these contributions [14, 21] :

- a) Vector exchange between strong/electromagnetic vertices with a weak transition in an external leg. These are usually called *indirect* amplitudes and they are model independent due to our good knowledge of the strong and electromagnetic processes involving vector mesons.
- b) The *direct* transitions are those where the weak vertices involving resonances are present and our poor knowledge of weak decays of resonances makes necessary the use of models in order to predict them.

The *indirect* model independent vector contribution corresponds to the diagrams in Fig. 3 that give (assuming $m_\pi = 0$)

$$M_{ind}^{(6)} = -\frac{G_8 e m_K^3}{2\pi^2 F_\pi} r_V [1 - 3z_3] , \quad (37)$$

$$r_V = \frac{64\sqrt{2}\pi^2 g_V h_V m_K^2}{3m_V^2} \simeq 0.41 ,$$

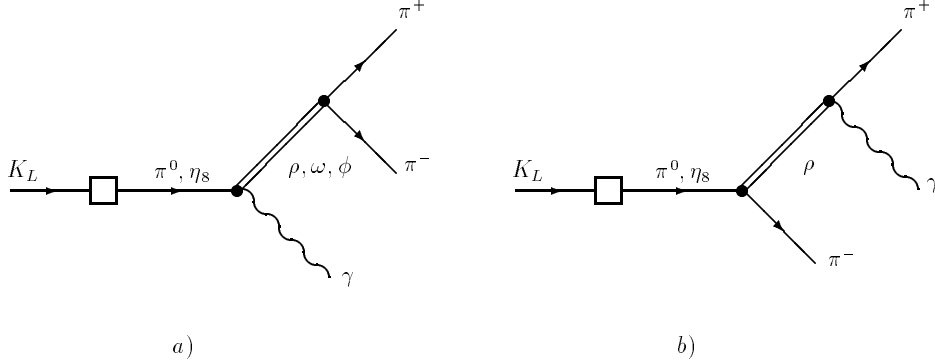


Figure 3: Diagrams contributing to the *indirect* vector meson exchange magnetic amplitude $M_{ind}^{(6)}$. The empty box is generated by $\mathcal{L}_2^{|\Delta S|=1}$ in Eq. (14) and the black circles by the strong/electromagnetic lagrangians \mathcal{L}_V in Eq. (10). In b) the crossed diagram $\pi^+ \leftrightarrow \pi^-$ has to be considered too.

where the numerical value of r_V is for $m_V = m_\rho$ ⁷. The strong/electromagnetic vertices present in the diagrams in Fig. 3 are given by the lagrangian density \mathcal{L}_V in Eq. (10). Several points are worth to comment: a) $M_{ind}^{(6)}$ shows a dependence in z_3 (i.e. in the photon energy); b) contrarily to what happened in the reducible anomalous contributions (Fig. 1.b and Fig. 2), even considering only the π^0 and the η_8 states, $M_{ind}^{(6)}$ does not vanish and our result agrees with the one quoted in Ref. [7].

Both contributions $M_{anom}^{(6)}$ and $M_{ind}^{(6)}$ are characterized by a weak transition in the external legs given by $\mathcal{L}_2^{|\Delta S|=1}$ in Eq. (14). We do not consider the Feynman diagrams where this transition happens in a pion final leg because they are suppressed by m_π^2/m_K^2 over those where the weak vertex happens in the initial K_L leg.

The *direct* resonance exchange contributions are generated by the diagrams in Fig. 4 where a direct weak vertex involving vector mesons is present. Due to our ignorance on these vertices from the phenomenological point of view it is necessary to invoke models in order to predict them. Moreover it has been shown [14, 21] that these contributions are

⁷If we include the singlet η_0 and η - η' mixing in Fig. 3 we would have found an extra term

$$\widetilde{M}_{ind}^{(6)} = \frac{G_{sem}^3}{2\pi^2 F_\pi} r_V F_1 \left[\frac{3}{2} - 3z_3 \right], \quad (38)$$

to be added to $M_{ind}^{(6)}$ in Eq. (37) (F_1 has been defined in Eq. (35)). However this term starts to contribute at $\mathcal{O}(p^8)$ and therefore is out of our scope here.

not small compared with the *indirect* ones and therefore have to be taken into account.

Thus we construct the most general weak $\mathcal{O}(p^3)$ Vector-Pseudoscalar-Photon ($VP\gamma$) and $\mathcal{O}(p^3)$ Vector-Pseudoscalar-Pseudoscalar (VPP) vertices appearing in the diagrams in Fig. 4 and then predict their couplings in the FMV model.

The most general $\mathcal{O}(p^3)$ weak octet $VP\gamma$ vertex for the processes of our interest has been already worked out in Ref. [14] and it is

$$\mathcal{L}_W(VP\gamma) = G_8 F_\pi^2 \langle V^\mu \mathcal{J}_\mu^W \rangle, \quad (39)$$

with

$$\mathcal{J}_\mu^W = \varepsilon_{\mu\nu\alpha\beta} \sum_{j=1}^5 \kappa_j T_j^{\nu\alpha\beta}, \quad (40)$$

and

$$\begin{aligned} T_1^{\nu\alpha\beta} &= \{ u^\nu, \Delta f_+^{\alpha\beta} \}, \\ T_2^{\nu\alpha\beta} &= \{ \{ \Delta, u^\nu \}, f_+^{\alpha\beta} \}, \\ T_3^{\nu\alpha\beta} &= \langle u^\nu \Delta \rangle f_+^{\alpha\beta}, \\ T_4^{\nu\alpha\beta} &= \langle u^\nu f_+^{\alpha\beta} \rangle \Delta, \\ T_5^{\nu\alpha\beta} &= \langle \Delta u^\nu f_+^{\alpha\beta} \rangle. \end{aligned} \quad (41)$$

In the same way the most general $\mathcal{O}(p^3)$ weak octet VPP vertex, without including mass terms, is

$$\mathcal{L}_W(VPP) = G_8 F_\pi^2 \langle V^{\mu\nu} \mathcal{J}_{\mu\nu}^W \rangle, \quad (42)$$

with

$$\mathcal{J}_{\mu\nu}^W = \sum_{j=1}^3 \sigma_j S_{\mu\nu}^j, \quad (43)$$

and

$$\begin{aligned} S_{\mu\nu}^1 &= i \{ u_\mu u_\nu, \Delta \}, \\ S_{\mu\nu}^2 &= i u_\mu \Delta u_\nu, \\ S_{\mu\nu}^3 &= i \langle \Delta u_\mu u_\nu \rangle. \end{aligned} \quad (44)$$

In Eqs. (40) and (43), the κ_i and σ_i are the *a priori* unknown coupling constants to be predicted in a model or given by the phenomenology when available.

With the weak vertices in $\mathcal{L}_W(VP\gamma)$ and $\mathcal{L}_W(VPP)$ and the strong/electromagnetic vertices given by \mathcal{L}_V in Eq. (10) we can compute now the diagrams in Fig. 4 and we get the direct contribution to the magnetic amplitude as given by vector meson dominance in terms of the κ_i and σ_i couplings

$$\begin{aligned} M_{dir}^{(6)} &= \frac{16}{3\sqrt{2}} \frac{G_8 e m_K^5}{m_V^2 F_\pi} \left\{ g_V [2\kappa_2 + 3\kappa_3 - (5\kappa_2 + 6\kappa_3) z_3] \right. \\ &\quad \left. - \sqrt{2} h_V [2\sigma_1 - (5\sigma_1 + \sigma_2) z_3] \right\}. \end{aligned} \quad (45)$$

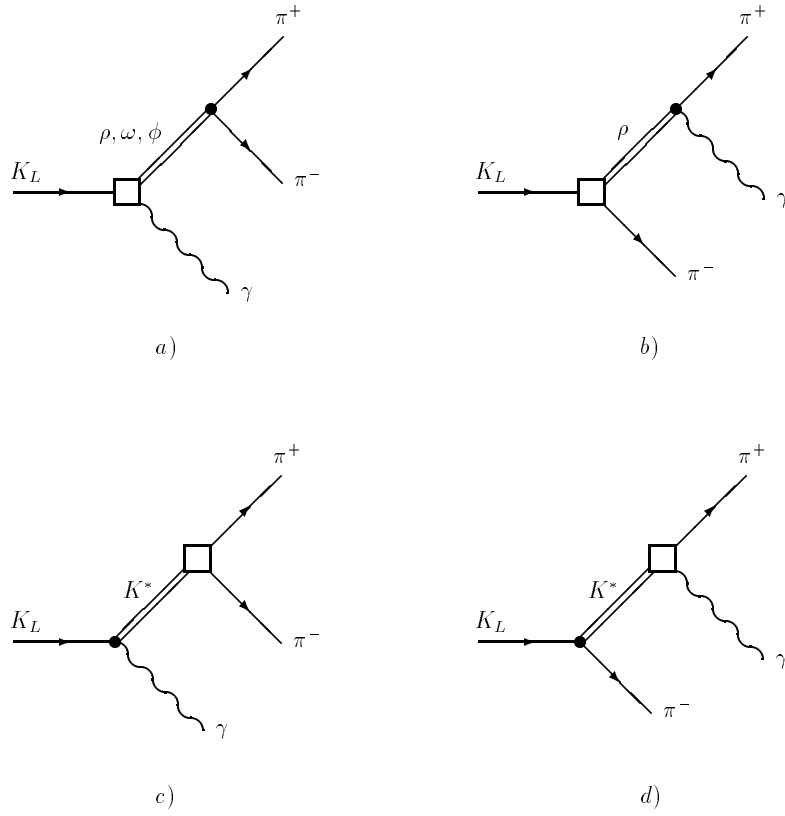


Figure 4: Diagrams contributing to the *direct* vector meson exchange magnetic amplitude $M_{dir}^{(6)}$. The empty box is generated by $\mathcal{L}_W(VP\gamma)$ in Eq. (39) or $\mathcal{L}_W(VPP)$ in Eq. (42) and the black circles by the strong/electromagnetic lagrangians \mathcal{L}_V in Eq. (10). In b) and d) the crossed $\pi^+ \leftrightarrow \pi^-$ diagrams are also understood.

In Ref. [14] we have proposed a Factorization Model in the Vector couplings that has proven to be very efficient in the understanding of the vector meson contributions to the $K \rightarrow \pi\gamma\gamma$ and $K_L \rightarrow \gamma\gamma^*$ processes. The prediction for κ_i in the FMV model has been worked out in Ref. [14]. To evaluate the σ_i we proceed analogously by applying factorization to construct the weak VPP vertex. A detailed evaluation is shown in Appendix B. The predictions for the coupling constants in this model are

$$\begin{aligned}
\kappa_1^{FMV} &= 0 & ; & \\
\kappa_2^{FMV} &= (2h_V - \ell_V) \eta_{VP\gamma} & ; & \quad \sigma_1^{FMV} = \frac{f_V}{\sqrt{2}} \left(\eta_V + 4L_9 \frac{m_V^2}{F^2} \eta_{VPP} \right) , \\
\kappa_3^{FMV} &= -\frac{8}{3} h_V \eta_{VP\gamma} & ; & \quad \sigma_2^{FMV} = -\sqrt{2} f_V \eta_V , \\
\kappa_4^{FMV} &= 2\ell_V \eta_{VP\gamma} & ; & \quad \sigma_3^{FMV} = -\sqrt{2} f_V \left(\eta_V + 2L_9 \frac{m_V^2}{F^2} \eta_{VPP} \right) , \\
\kappa_5^{FMV} &= 2\ell_V \eta_{VP\gamma} & ; &
\end{aligned} \tag{46}$$

where

$$\ell_V = \frac{3}{16\sqrt{2}\pi^2} f_V \frac{m_V^2}{F^2} \simeq 4h_V , \tag{47}$$

and the last identity is exact in the Hidden gauge model and also well supported phenomenologically. As explained in Ref. [14], ℓ_V is a contribution given by the $\mathcal{O}(p^4)$ WZW anomaly Eq.(7). In Eq. (46) the unknown factorization factors are $\eta_{VP\gamma}$ that comes from the $\mathcal{O}(p^3)$ weak $VP\gamma$ vertex, η_{VPP} from the $\mathcal{O}(p^3)$ weak VPP vertex and η_V from an $\mathcal{O}(p)$ weak PV vertex [26] (see also Appendix B) and that we already have met in the predictions for N_i^{V+A} in Eq. (25). Naive factorization, however, would put $\eta_{VP\gamma} = \eta_{VPP} = \eta_V$. In Ref. [14] we have shown that the phenomenology of $K \rightarrow \pi\gamma\gamma$ and $K_L \rightarrow \gamma\gamma^*$ is well described with $\eta_{VP\gamma} \simeq 0.21$ as predicted by the naive Wilson coefficient in Eq. (21) (i.e. no enhancement of the $\Delta I = 1/2$ transitions) and we will use this result in our numerical study. For η_{VPP} and η_V we do not have still any information. However we will assume $\eta_{VPP} \simeq \eta_{VP\gamma}$ because of factorization and we will leave η_V free. This is because while η_{VPP} and $\eta_{VP\gamma}$ appear both at $\mathcal{O}(p^3)$ in the weak chiral lagrangian, η_V appears at $\mathcal{O}(p)$ and therefore could differ appreciably from the naive result.

With the FMV predictions for the couplings κ_i and σ_i we can give the direct $M_{dir}^{(6)}$ amplitude in this model. Substituting in Eq. (45) we get

$$\begin{aligned}
M_{dir,FMV}^{(6)} &= -\frac{G_8 e m_K^3}{2\pi^2 F_\pi} r_V \left[(\eta_{VP\gamma} + \eta_V) \left(1 - \frac{3}{2} z_3\right) \right. \\
&\quad \left. + \eta_{VP\gamma} \frac{\ell_V}{4h_V} (2 - 5z_3) \right. \\
&\quad \left. + 2\eta_{VPP} L_9 \frac{m_V^2}{F^2} (2 - 5z_3) \right] , \tag{48}
\end{aligned}$$

where r_V has been defined in Eq. (37), ℓ_V in Eq. (47) and we have put $m_\pi = 0$. Note that $M_{dir}^{(6)}$ gets a dependence on the photon energy.

Another procedure to implement the hypothesis of factorization has also been used in the literature [7, 21]. In this case one determines first the strong action generated by vector meson dominance and then applies the FM as given by Eq. (23). This is the so called procedure \mathcal{A} [12, 26] in opposition to the FMV model where one first determines in Factorization the weak couplings of vectors and then integrate them out (procedure \mathcal{B}).

According to the method \mathcal{A} the vector generated $\mathcal{O}(p^6)$ strong action necessary to compute the direct magnetic amplitude for $K_L \rightarrow \pi^+\pi^-\gamma$ has two contributions : i) the one given by integrating the vector mesons between the terms in g_V and h_V in \mathcal{L}_V (Eq. (10)), and ii) a term obtained by integrating the vectors between the terms in f_V and h_V in Eq. (10). Once factorization is applied these generate the following magnetic amplitude :

$$M_{dir,FM}^{(6)} = -\frac{G_8 e m_K^3}{2\pi^2 F_\pi} r_V k_F \left[(2 - 3z_3) + \frac{f_V}{2g_V} (2 - 5z_3) \right], \quad (49)$$

where r_V has been defined in Eq. (37) and k_F is the factorization parameter. In $M_{dir,FM}^{(6)}$ the term proportional to f_V is the one given by the second contribution (ii) above. In Ref. [7] only the term generated by the first structure (i) has been considered.

The theoretical comparison between the two models motivates the following considerations.

- 1) As has been shown in Ref. [14] the FM and FMV models do not give the same contributions. In fact the FMV model recovers the results of the FM but it is able to generate a more complete set of effective operators. The fact that one recovers more chiral operators in the FMV model was shown to be important in Ref. [14] for the understanding of the vector meson contributions to $K \rightarrow \pi\gamma\gamma$ and $K_L \rightarrow \gamma\gamma^*$. In $K_L \rightarrow \pi^+\pi^-\gamma$ the weak VPP vertex generates an extra contribution (last line in Eq. (48)) that the FM does not get [7]⁸.
- 2) The σ_i^{FMV} couplings in the weak VPP vertex have two different kinds of contributions. From Eq. (46) we see that there is a term proportional to η_{VPP} and a piece proportional to η_V . The first one, analogous to the $\eta_{VP\gamma}$ contribution in κ_i^{FMV} , comes from the application of factorization through the left-handed currents in the direct VPP vertex. As explained in Appendix B the origin of the term proportional to η_V is a weak shift in the kinetic term of the vector fields in the conventional vector formulation. This framework, that we have proposed in Ref. [26], has been able to generate new features in the $\mathcal{O}(p^4)$ N_i couplings of $\mathcal{L}_4^{|\Delta S|=1}$ like, for example,

⁸In comparing our result $M_{dir,FMV}^{(6)}$ with the one given by the FM in Ref. [7] care has to be taken because the anomalous contribution given by the term proportional to L_9 in the FM (Eq. (5.24) of Ref. [7]) corresponds to our term proportional to ℓ_V in Eq. (48) and coincides with it once the relation $L_9 = f_V g_V / 2 = f_V^2 / 4$ is used.

non-vanishing spin-1 resonance exchange contributions to the N_{28}, \dots, N_{31} couplings in Eqs. (18,25) that are predicted to be zero in the FM with the antisymmetric formulation [12]. It is reassuring to notice that the term proportional to η_V allows us to recover the result of the FM [7] for $K_L \rightarrow \pi^+\pi^-\gamma$ (that is $\mathcal{O}(p^6)$) in agreement with our claim that the procedure we are applying uncovers new structures but does not miss any contained in the previous FM. This shows that our approach in Ref. [26] is also consistent at $\mathcal{O}(p^6)$ and hence with the chiral expansion.

We think that the FMV model seems to give a more complete description and therefore we will analyse the $K_L \rightarrow \pi^+\pi^-\gamma$ process in this model.

Using the relations $\ell_V = 4h_V$ (Eq. (47)) and $L_9 = f_V^2/4$ we can give a simplified expression for $M_{dir,FMV}^{(6)}$,

$$M_{dir,FMV}^{(6)} = -\frac{G_8 e m_K^3}{2\pi^2 F_\pi} r_V \eta_{VP\gamma} \left[3 + 2\omega + \omega' - \frac{1}{2} (13 + 10\omega + 3\omega') z_3 \right], \quad (50)$$

where $\omega = \eta_{VPP}/\eta_{VP\gamma}$, $\omega' = \eta_V/\eta_{VP\gamma}$ and naive factorization would suggest $\omega = \omega' = 1$. However, as commented before, we would like to emphasize that while the value of $\eta_{VP\gamma} \simeq 0.21$ has been fixed in Ref. [14] from the phenomenology of $K \rightarrow \pi\gamma\gamma$ and $K_L \rightarrow \gamma\gamma^*$, no similar constraint affects η_{VPP} or η_V and it could happen that, in contradistinction with $\eta_{VP\gamma}$, these weak vertices are affected by the $\Delta I = 1/2$ enhancement and therefore ω and ω' could differ appreciably from the unity. It is worth to notice that, in principle, both contributions to $M_{dir,FMV}^{(6)}$ coming from the weak $VP\gamma$ (the pure numerical term in the brackets in Eq. (50)) and VPP vertices (terms in ω and ω') are quantitatively comparable and of the same order. Thus we find that the phenomenological assumption by Heiliger and Sehgal [36] that the vector exchange generated DE amplitude of $K_L \rightarrow \pi^+\pi^-\gamma$ is dominated by the weak $VP\gamma$ vertex as in $K \rightarrow \pi\gamma\gamma$ and $K_L \rightarrow \gamma\gamma^*$, is not supported by our analysis.

Moreover, comparing $M_{dir,FMV}^{(6)}$ and $M_{ind}^{(6)}$ in Eq. (37) we also see that both *direct* and *indirect* contributions are comparable as it happens in $K \rightarrow \pi\gamma\gamma$ and $K_L \rightarrow \gamma\gamma^*$.

4.2 Loop amplitudes

The leading loop contributions to the magnetic amplitude of $K_L \rightarrow \pi^+\pi^-\gamma$ are $\mathcal{O}(p^6)$ in χ PT. There are two different kinds of loop generated amplitudes.

The first type corresponds to the Feynman diagrams in Fig. 5 which contribution is given by the lagrangian densities $\mathcal{L}_2^{|\Delta S|=1}$ in Eq. (14), the strong/electromagnetic \mathcal{L}_2 in Eq. (3) and the WZW anomalous action $Z_{an}[U, \ell, r]_{WZW}$ in Eq. (7). Thus the main feature is that this contribution is completely specified on chiral symmetry and anomaly grounds and, therefore, it is model independent.

In Fig. 5.a the fields running in the loop are the pairs (η_8, π^\pm) and (π^0, π^\pm) . In the pole-like diagrams in Figs. 5.b-5.e we keep those where the external kaon leg undergoes

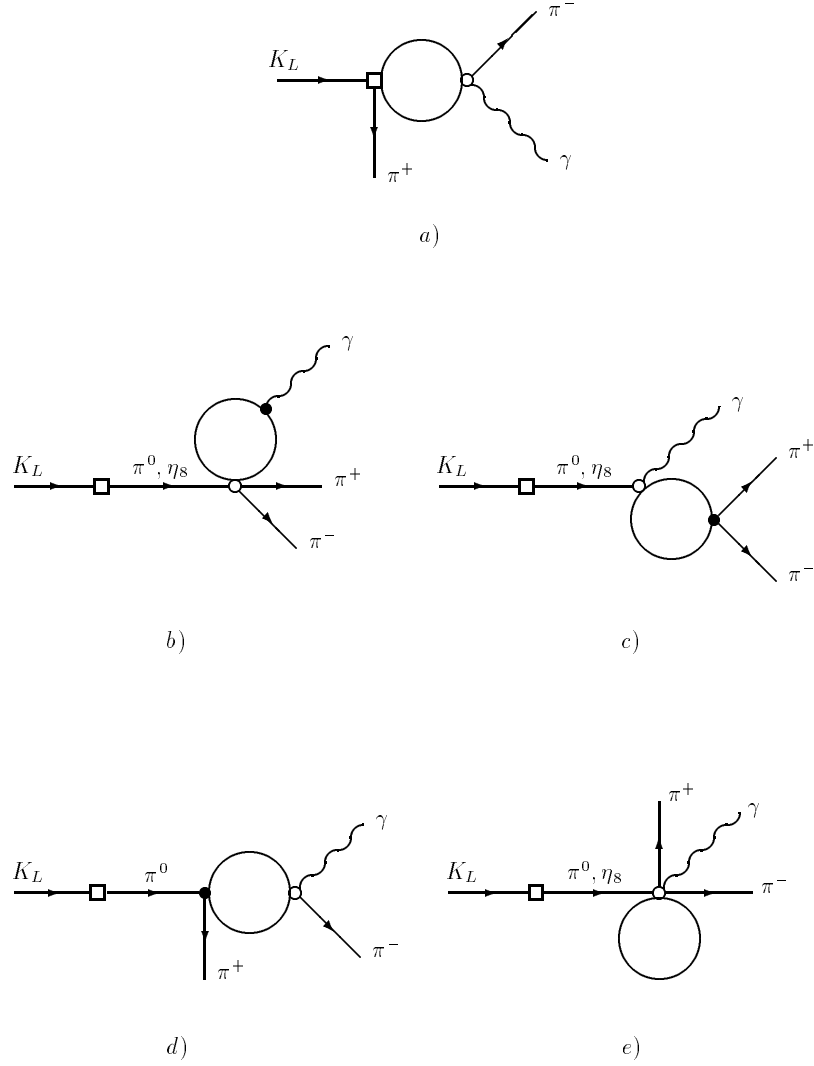


Figure 5: Diagrams contributing to the *loop* magnetic amplitude $M_{WZW}^{(6)}$. The empty box is generated by $\mathcal{L}_2^{|\Delta S|=1}$ in Eq. (14), the white circles by the WZW anomalous action Z_{an} in Eq. (7) and the black circles by the strong/electromagnetic lagrangian \mathcal{L}_2 in Eq. (3). In a) and d) the crossed $\pi^+ \leftrightarrow \pi^-$ diagrams are also taken into account.

the weak transition to π^0 , η_8 and disregard those (suppressed by m_π^2/m_K^2) where the transition happens in a final leg. In the diagram in Fig. 5.b only K^+ is running in the loop and its final contribution vanishes because a cancellation between the π^0 and the η_8 ; in Fig. 5.c we have π^+, K^+, K^0 ; in Fig. 5.d the couple (π^\pm, π^0) and in Fig. 5.e we have π^+, π^0, K^+ and K^0 . We note also that there is no pole contribution with η_8 in the diagram in Fig. 5.d.

The result is divergent and in the \overline{MS} subtraction scheme is

$$\begin{aligned}
M_{WZW}^{(6)} = & \frac{G_8 e m_K^3}{2\pi^2 F_\pi} \left(\frac{m_K}{4\pi F_\pi} \right)^2 \left[\frac{5}{9} r_\pi^2 - \frac{5}{9} + \frac{7}{3} r_\pi^2 \ln \left(\frac{m_\pi^2}{\mu^2} \right) - \frac{7}{3} \ln \left(\frac{m_K^2}{\mu^2} \right) \right. \\
& + \left[\frac{5}{3} - \frac{2}{3} \ln \left(\frac{m_K^2}{\mu^2} \right) - \frac{1}{3} \ln \left(\frac{m_\pi^2}{\mu^2} \right) \right] z_3 \\
& + K[(p-p_+)^2, m_\pi^2, m_\pi^2] + K[(p-p_-)^2, m_\pi^2, m_\pi^2] \\
& + \frac{2}{3} K[(p-p_+)^2, m_\pi^2, m_\eta^2] + \frac{2}{3} K[(p-p_-)^2, m_\pi^2, m_\eta^2] \\
& + \frac{2}{3} r_\pi^2 \left(F[(p-p_+)^2, m_\pi^2] + F[(p-p_-)^2, m_\pi^2] \right) \\
& \left. - \frac{4}{3} F[(p_+ + p_-)^2, m_K^2] \right], \tag{51}
\end{aligned}$$

where the functions $F[q^2, m^2]$ and $K[q^2, m_1^2, m_2^2]$ have been defined in the Appendix C.

We have compared the loop evaluation of $\pi^0 \rightarrow \pi^+ \pi^- \gamma$ and $\eta_8 \rightarrow \pi^+ \pi^- \gamma$ (necessary for the pole-like diagrams in Fig. 5) with the results shown in the Ref. [37] and found complete agreement. From our Eq. (51) it is easier to obtain the appropriate momentum dependence that is not properly specified in Ref. [37]. Moreover the divergent part of these diagrams comes from the strong/electromagnetic loop because the weak transition happens in the external leg. We have checked, then, that the strong intrinsic parity violating $\mathcal{O}(p^6)$ lagrangian [38] can absorb these divergences.

The second type of loop contributions corresponds to the Feynman diagrams in Fig. 6. Their basic characteristic is that the weak vertices are generated by $\mathcal{L}_4^{|\Delta S|=1}$ in Eq. (18) and therefore the generated amplitudes are proportional to the, a priori unknown, N_i couplings. The strong vertices in Fig. 6 are generated by \mathcal{L}_2 in Eq. (3). In Fig. 6.a the fields running in the loop are the pairs (π^+, π^-) and (K^+, K^-) ; in Fig. 6.b we have $\pi^+, \pi^0, \eta_8, K^0$ and K^+ ; finally in the graph in Fig. 6.c there are the pairs (K^0, π^\pm) , (K^\pm, π^0) and (K^\pm, η_8) . We also have taken into account the field and F_π renormalization due to the leading $M^{(4)}$ amplitude in Eq. (31).

As in the case above the result is divergent and using the \overline{MS} scheme it reads

$$\begin{aligned}
M_{N_i}^{(6)} = & \frac{G_8 e m_K^3}{2\pi^2 F_\pi} \left(\frac{m_K}{4\pi F_\pi} \right)^2 (8\pi^2) \cdot \\
& \left\{ 3 N_{28} \ln \left(\frac{m_K^2}{\mu^2} \right) \right. \tag{52}
\end{aligned}$$

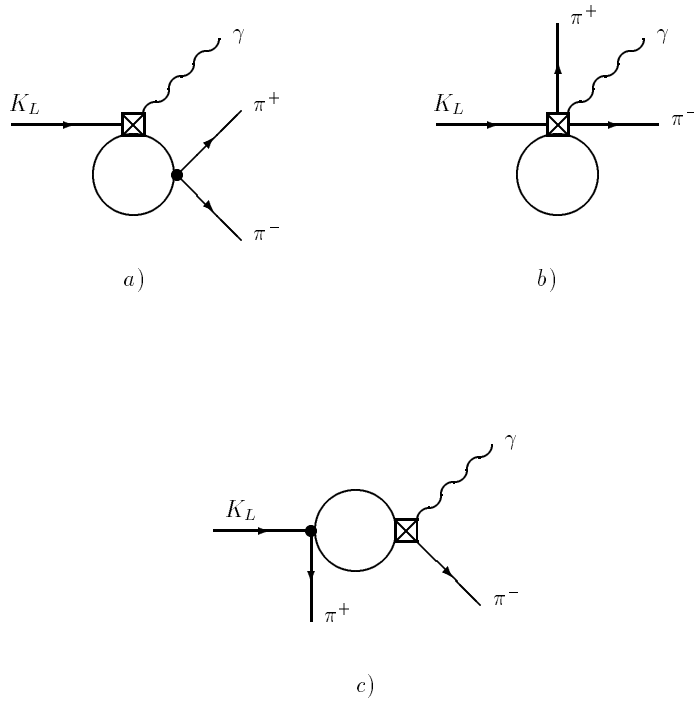


Figure 6: Diagrams contributing to the *loop* magnetic amplitude $M_{N_i}^{(6)}$. The crossed box is generated by $\mathcal{L}_4^{|\Delta S|=1}$ in Eq. (18), and the black circles by the strong lagrangian \mathcal{L}_2 in Eq. (3). In c) the crossed $\pi^+ \leftrightarrow \pi^-$ diagram is also considered.

$$\begin{aligned}
& + (3N_{29} - N_{30}) \left[2 \ln \left(\frac{m_K^2}{\mu^2} \right) + K[(p - p_+)^2, m_K^2, m_\pi^2] \right. \\
& \quad + K[(p - p_-)^2, m_K^2, m_\pi^2] + K[(p - p_+)^2, m_K^2, m_\eta^2] \\
& \quad \left. + K[(p - p_-)^2, m_K^2, m_\eta^2] \right] \\
& + 2 (N_{29} + N_{31}) \left[-\frac{5}{6} + \left(\frac{15}{4} r_\pi^2 + \frac{1}{3} \right) \ln \left(\frac{m_\pi^2}{\mu^2} \right) + \frac{8}{3} \ln \left(\frac{m_K^2}{\mu^2} \right) \right. \\
& \quad + \frac{3}{4} r_\eta^2 \ln \left(\frac{m_\eta^2}{\mu^2} \right) + \left[\frac{5}{3} - \frac{2}{3} \ln \left(\frac{m_\pi^2}{\mu^2} \right) - \frac{1}{3} \ln \left(\frac{m_K^2}{\mu^2} \right) \right] z_3 \\
& \quad - \frac{4}{3} r_\pi^2 F[(p_+ + p_-)^2, m_\pi^2] - \frac{2}{3} F[(p_+ + p_-)^2, m_K^2] \\
& \quad \left. + K[(p - p_+)^2, m_K^2, m_\pi^2] + K[(p - p_-)^2, m_K^2, m_\pi^2] \right] \Big\} ,
\end{aligned}$$

and the functions $F[q^2, m^2]$ and $K[q^2, m_1^2, m_2^2]$ have been defined in the Appendix C.

We notice that $M_{N_i}^{(6)}$ depends on the four N_{28}, \dots, N_{31} unknown couplings in the $\mathcal{O}(p^4)$ weak lagrangian, but only three combinations of them, N_{28} , $3N_{29} - N_{30}$ and $N_{29} + N_{31}$, appear.

In our numerical study of the branching ratio and spectrum in the next section we have worked with the full expressions of $M_{WZW}^{(6)}$ and $M_{N_i}^{(6)}$ with $\mu = m_\rho$. However in order to make more transparent our study of the slope in $K_L \rightarrow \pi^+ \pi^- \gamma$ (Eq. (32)) we have linearized the real part of the loop contributions by Taylor expanding the amplitude assuming $4r_\pi^2 \leq z_3 \ll 1$. We get for the full $\mathcal{O}(p^6)$ loop contribution

$$M_{Loop}^{(6)} = \frac{G_8 e m_K^3}{2\pi^2 F_\pi} \left(\frac{m_K}{4\pi F_\pi} \right)^2 [a_L + b_L z_3] , \quad (53)$$

where

$$a_L = 2.51 - 2.63 a_1 - 2.07 (a_2 + 2a_4) - 0.13 (a_2 - 2a_3) , \quad (54)$$

$$b_L = 0.50 + 0.67 (a_2 + 2a_4) - 0.07 (a_2 - 2a_3) .$$

The linearizations give values for $Re(M_{Loop}^{(6)})$ in very good agreement with the exact results (in a very few percent inside the domain of z_3). From Eq. (54) we notice that if $a_i \sim \mathcal{O}(1)$ (as expected) the main contributions come from the model independent amplitude and the terms in $a_1 \propto N_{28}$ and $(a_2 + 2a_4) \propto (N_{29} + N_{31})$.

5 Analysis of $K_L \rightarrow \pi^+ \pi^- \gamma$

Collecting all our previous results for the magnetic amplitude of $K_L \rightarrow \pi^+ \pi^- \gamma$ (with the linearized version of the loop contributions) we get for the factor \widetilde{m} and the slope c

defined in Eq. (32) the results

$$\widetilde{m} = a_2 + 2a_4 - F_1 + r_V [1 + \eta_{VP\gamma} (3 + 2\omega + \omega')] - \left(\frac{m_K}{4\pi F_\pi}\right)^2 a_L, \quad (55)$$

$$c = -\frac{1}{\widetilde{m}} \left[r_V \left(3 + \frac{\eta_{VP\gamma}}{2} (13 + 10\omega + 3\omega') \right) + \left(\frac{m_K}{4\pi F_\pi}\right)^2 b_L \right]. \quad (56)$$

We recall here what is known and what is not in the expressions above:

- a) The $\mathcal{O}(p^4)$ $a_2 + 2a_4$ term is unknown. In Subsection 2.2 we have given the predictions for a_i in the FM (anomaly) and the vector formulation framework using factorization (spin-1 resonances) in terms of one free parameter η . We will study our observables in a reasonable range of this term : $0 < a_2 + 2a_4 \leq 3$ (we remind that factorization predicts $a_i \sim \mathcal{O}(1)$ and positive).
- b) F_1 has been defined in Eq. (35) and the only parameter we will allow to be free is the one measuring the breaking of the nonet symmetry in the weak vertex ρ defined in Eq. (17). We will consider $0 \leq \rho \leq 1$ as a conservative working region.
- c) r_V is given in Eq. (37); $\eta_{VP\gamma}$ has been fixed in Ref. [14] to $\eta_{VP\gamma} \simeq 0.21$ as commented before.
- d) The ratio $\omega = \eta_{VPP}/\eta_{VP\gamma}$, defined in Eq. (50), is also free and we will allow a domain $0.5 \leq \omega \leq 1.5$ coherently with the naive estimate of factorization that sets $\omega \simeq 1$. However we will keep free $\omega' = \eta_V/\eta_{VP\gamma}$ and will allow a reasonable range of values for η_V , i.e. $0 < \eta_V \leq 1$.
- e) The a_L and b_L parameters have been defined in Eq. (54) and therefore they depend on the unknown a_i couplings. Our procedure will be the following. For every value of the $\mathcal{O}(p^4)$ $a_2 + 2a_4$ free parameter we use the results in Eqs. (24,25) with $\eta_V = \eta_{an} \equiv \eta$ to fix a value for η as given by

$$\eta = \frac{a_2 + 2a_4}{3 + \frac{32\pi^2}{\sqrt{2}} f_V h_V}. \quad (57)$$

With this value then we fix a_1 and $a_2 - 2a_3$ that appear in the loop contributions. For definiteness we have not included the axial contribution in N_i and therefore in Eq. (57). If included it would add constructively in the denominator giving a smaller value of η . From Eq. (54) we see that the dependence of the loop contribution in $a_2 - 2a_3$ is very mild and only a_1 is relevant. Values for a_L and b_L for fixed $a_2 + 2a_4$ are collected in Table 1. We notice that while a_L even changes sign with the running of $a_2 + 2a_4$, the slope term b_L grows steadily.

$a_2 + 2a_4$	0.4	0.6	0.8	1.0	1.2	1.4
a_L	1.12	0.42	-0.27	-0.97	-1.66	-2.36
b_L	0.77	0.91	1.05	1.19	1.33	1.47

Table 1: Loop contributions a_L and b_L in Eqs. (53,54) for different values of the $a_2 + 2a_4$ parameter as explained in the text.

We have therefore three, a priori, free parameters : ρ , ω and $a_2 + 2a_4$. Using now the experimental values for the branching ratio and the slope of $K_L \rightarrow \pi^+\pi^-\gamma$ we can proceed to the analysis. However there is another process where the breaking of the nonet symmetry in the weak sector could play a rôle : $K_L \rightarrow \gamma\gamma$. A short note on this process is now needed.

$K_L \rightarrow \gamma\gamma$ is a decay dominated by long-distance contributions which first non vanishing amplitude is $\mathcal{O}(p^6)$ in χ PT [39, 40]. Neglecting CP violating effects the amplitude is defined by

$$A[K_L(p) \rightarrow \gamma(q_1, \epsilon_1)\gamma(q_2, \epsilon_2)] = i A_{\gamma\gamma} \epsilon_{\mu\nu\sigma\tau} \epsilon_1^\mu(q_1) \epsilon_2^\nu(q_2) q_1^\sigma q_2^\tau. \quad (58)$$

There is, up to now, no full computation at $\mathcal{O}(p^6)$ in χ PT. At present the amplitude is taken

$$A_{\gamma\gamma} = -\frac{2}{\pi} G_8 F_\pi \alpha_{em} F_2, \quad (59)$$

where

$$F_2 = \frac{1}{1-r_\pi^2} + \frac{1}{3(1-r_\eta^2)} [(1+\xi) \cos\theta + 2\sqrt{2}\rho \sin\theta] \left[\frac{F_\pi}{F_8} \cos\theta - 2\sqrt{2}\frac{F_\pi}{F_0} \sin\theta \right] - \frac{1}{3(1-r_{\eta'}^2)} [2\sqrt{2}\rho \cos\theta - (1+\xi) \sin\theta] \left[\frac{F_\pi}{F_8} \sin\theta + 2\sqrt{2}\frac{F_\pi}{F_0} \cos\theta \right], \quad (60)$$

comes from the pole-like diagrams with the same definitions than F_1 in Eq. (35)⁹. In our previous study on $K_L \rightarrow \gamma\gamma^*$ [14] we noticed that, keeping only the term in F_2 in

⁹In Ref. [41] has been pointed out an extra contribution to $A_{\gamma\gamma}$ coming precisely from a one loop evaluation using $\mathcal{L}_4^{|\Delta S|=1}$. We have not been able to recover that result and found the claimed new contribution vanishes, therefore we do not take it into account. After reviewing their calculation the authors of Ref. [41] now agree with us.

Eq. (59) with $\rho = 1$ and $F_\pi = F_8 = F_0$ all the vector meson dominance models known were giving a wrong sign for the slope in $K_L \rightarrow \gamma\gamma^*$. Due to the poor knowledge of the $K_L \rightarrow \gamma\gamma$ amplitude we think that the problem could be the sign of this amplitude. Using the experimental figure [20] $|A_{\gamma\gamma}^{exp}| = (3.51 \pm 0.05) \times 10^{-9} \text{ GeV}^{-1}$, from Eq. (59) we get $|F_2^{exp}| = 0.883 \pm 0.013$. We have fixed the range $0 \leq \rho \leq 1$ by the conservative assumption that $|F_2^{theor}|$ does not differ from the experimental figure more than a factor 2. We will include this process in our study and will combine, therefore, $K_L \rightarrow \gamma\gamma$ and $K_L \rightarrow \pi^+\pi^-\gamma$.

In our numerical analysis we use the following values for the known parameters: the mixing angle between η_8 and η_0 that appears in F_1 and F_2 is taken $\theta \simeq -20^\circ$; the $SU(3)$ breaking parameter ξ defined in Eq. (36) is $\xi \simeq 0.17$ [40]; the ratios between the decay constants are $F_\pi/F_8 \simeq 0.77$ [2] and $F_\pi/F_0 \simeq 0.98$ [42]¹⁰; the couplings defined in Eq. (10) are $f_V = 2g_V \simeq 0.18$, $h_V \simeq 0.037$ and $\theta_V = 2h_V$.

Our analysis shows the following features :

- 1/ There is a very mild dependence in the ω parameter for the indicated domain $0.5 \leq \omega \leq 1.5$. It gives an uncertainty in our predictions on $K_L \rightarrow \pi^+\pi^-\gamma$ of around 10% for the branching ratio and 5% for the slope. Hereafter we take $\omega = 1$ in our analysis.
- 2/ In Table 2 we show, for fixed values of a_2+2a_4 , the region in ρ that gives a reasonable result for $B(K_L \rightarrow \pi^+\pi^-\gamma ; E_\gamma^* > 20 \text{ MeV})_{DE}$, the prediction for the slope c in $K_L \rightarrow \pi^+\pi^-\gamma$ and the values of F_2 in $A_{\gamma\gamma}$. We see that the branching ratio can always be accommodated for reasonable values of a_2+2a_4 and ρ . Taking into account $|F_2|$ in $K_L \rightarrow \gamma\gamma$, however, there is a restriction on the lower and upper limits of $a_2 + 2a_4$, roughly $0.4 \leq a_2 + 2a_4 \leq 1.4$ and also an internal region of this interval is excluded because $|F_2|$ is too small. Thus the combined analysis of the experimental widths of $K_L \rightarrow \pi^+\pi^-\gamma$ and $K_L \rightarrow \gamma\gamma$ are consistent in two regions of parameters that are ruled only by the value of the combination $a_2 + 2a_4$:

$$\begin{aligned} \textbf{Region I} : \quad & 0.4 \leq a_2 + 2a_4 \leq 0.8 , \quad 0 \leq \rho \leq 0.4 , \\ & 0.09 \leq \eta \leq 0.18 , \quad F_2 < 0 ; \end{aligned}$$

$$\begin{aligned} \textbf{Region II} : \quad & 1.0 < a_2 + 2a_4 \leq 1.4 , \quad 0.6 < \rho \leq 1 , \\ & 0.22 < \eta \leq 0.31 , \quad F_2 > 0 . \end{aligned}$$

We remind that pion pole dominance in $K_L \rightarrow \gamma\gamma$ demands $F_2 > 0$. Our analysis, however, shows that both possibilities are consistent in the framework we have developed here, and that the breaking of the nonet symmetry in the $\mathcal{O}(p^2)$ weak

¹⁰These values are consistent with the recent analysis of Ref. [43].

$a_2 + 2a_4$	ρ	$B(K_L \rightarrow \pi^+\pi^-\gamma; E_\gamma^* > 20 \text{ MeV})_{DE} \times 10^5$	c	F_2
0.4	-0.05	3.86	-1.54	-1.89
	0.00	3.27	-1.63	-1.72
	0.05	2.73	-1.73	-1.55
0.6	0.15	3.78	-1.58	-1.22
	0.20	3.20	-1.67	-1.05
	0.25	2.67	-1.77	-0.89
0.8	0.35	3.71	-1.61	-0.55
	0.40	3.13	-1.70	-0.39
	0.45	2.61	-1.81	-0.22
1.0	0.55	3.64	-1.64	0.11
	0.60	3.07	-1.74	0.28
	0.65	2.55	-1.84	0.45
1.2	0.75	3.56	-1.67	0.79
	0.80	3.00	-1.77	0.95
	0.85	2.49	-1.88	1.11
1.4	0.95	3.49	-1.71	1.45
	1.00	2.94	-1.80	1.61
	1.05	2.43	-1.91	1.78

Table 2: Range of values of ρ that give a reasonable prediction for the branching ratio and the slope of $K_L \rightarrow \pi^+\pi^-\gamma$ at fixed value of $a_2 + 2a_4$ for $\omega = 1$. The prediction for F_2 is also given. The experimental values are $B(K_L \rightarrow \pi^+\pi^-\gamma; E_\gamma^* > 20 \text{ MeV})_{DE} = (3.19 \pm 0.16) \times 10^{-5}$, $c_{exp} = -1.7 \pm 0.5$ and $|F_2| = 0.883 \pm 0.013$.

vertex could consistently be as big as $\rho \simeq 0.2$. Notice that if we had included the axial-vector contribution in the determination of η in Eq. (57) this parameter would diminish by a 15%.

- 3/ As can be seen in Table 2 the predicted slope c of $K_L \rightarrow \pi^+\pi^-\gamma$ is in a small range $c \simeq -1.6, -1.8$, independently from the range of parameters and in excellent agreement with the experimental figure $c_{exp} = -1.7 \pm 0.5$. As seen from Eq. (56) the slope has two contributions : vector exchange and loops. The rôle of the latter is crucial in stabilizing the prediction. This can be seen in Table 3 where we show the values of the slope including only the vector amplitude ($c \simeq -1.4, -2.3$) and the total result obtained by adding the loop contribution ($c \simeq -1.6, -1.8$). The corrections to the width coming from the loop amplitudes are mainly relevant in

$a_2 + 2a_4$	0.4	0.6	0.8	1.0	1.2	1.4
ρ	0.0	0.2	0.4	0.6	0.8	1.0
c (vectors only)	-1.36	-1.48	-1.63	-1.81	-2.02	-2.28
c (vectors + loops)	-1.63	-1.67	-1.70	-1.74	-1.77	-1.80

Table 3: Comparison between the values of the slope c of the magnetic amplitude of $K_L \rightarrow \pi^+\pi^-\gamma$ for a fixed value of $a_2 + 2a_4$ as given by vector exchange only and adding the loop contributions in the total result. When the latter are included the prediction is much more steady.

Region II where can reach even 100% for $a_2 + 2a_4 = 1.2$. This is because in this region there is an almost complete cancellation of the term $a_2 + 2a_4 - F_1$ of \tilde{m} in Eq. (55) and thus providing instability to the result; axial-vector exchange or higher $\mathcal{O}(p^8)$ corrections, not included in this analysis, might then be relevant. In Region I the loop contribution to the branching ratio is never bigger than 20%.

In Fig. 7 we plot the spectrum of the *direct emission* $K_L \rightarrow \pi^+\pi^-\gamma$ in the photon energy (E_γ^*) for the two extreme values $a_2 + 2a_4 = 0.4$ (Region I) with $\rho = 0$, $c = -1.63$, and $a_2 + 2a_4 = 1.4$ (Region II) with $\rho = 1$, $c = -1.80$. The tiny difference between both curves shows the model dependence of our prediction. We have normalized the spectrum to the 1937 events reported by the E731 experiment in Ref. [35] that are also displayed. From this Fig. 7 it would seem that a bigger value of the magnitude of the slope (and thus shifting the spectrum to lower values of E_γ^*) is needed. This could be accommodated in our framework through other resonance exchange at $\mathcal{O}(p^6)$ (like axial-vector mesons) or $\mathcal{O}(p^8)$ corrections. Due to the experimental uncertainties is however premature to reach such a conclusion and a further improvement from the experimental side would be very much welcome.

In Ref. [44] a parameter f measuring the fraction of the $\Delta I = 1/2$ $K \rightarrow \pi\pi$ amplitude due to penguin effects was introduced. This ratio can be related with the parameter ρ introduced in Eq. (17) that measures the breaking of the nonet symmetry in the weak sector through the relation (assuming CP conserved) $\rho = (3f - 1)/2$ [44]. There are a lot

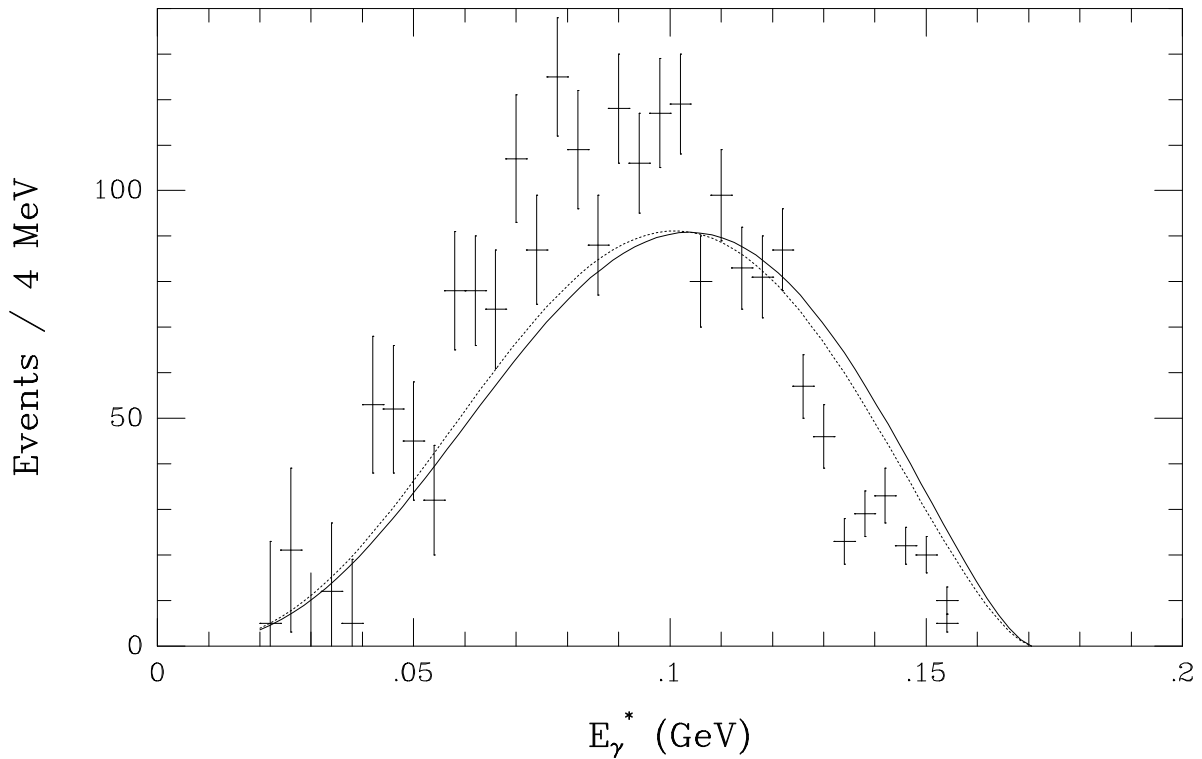


Figure 7: Spectrum in E_γ^* ($E_\gamma^* > 20$ MeV) of the $K_L \rightarrow \pi^+ \pi^- \gamma$ (DE) process normalized to the 1937 events of the E731 experiment of Ref. [35] that are also displayed. The continuous line corresponds to $a_2 + 2a_4 = 0.4$, $\rho = 0$ and $\omega = 1$ with a predicted slope of $c = -1.63$. The dotted line corresponds to $a_2 + 2a_4 = 1.4$, $\rho = 1$ and $\omega = 1$ with a predicted slope of $c = -1.80$.

of uncertainties in the determination of f and little can be said. We just recall that for the generous range $0.1 \leq f \leq 0.8$ it implies $-0.2 \leq \rho \leq 0.7$. Coming back to our analysis we see that Region I implies $0.3 \leq f \leq 0.6$ while Region II allows $0.7 \leq f \leq 1$ in the boundary of the reasonable range.

A joint analysis of $K_L \rightarrow \pi^+\pi^-\gamma$ and $K_L \rightarrow \gamma\gamma$ has also been carried out previously by other authors. Cheng [31, 45] only includes the term $a_2 + 2a_4 - F_1$ in \widetilde{m} (Eq. (55)) and, moreover, arbitrarily input $a_2 = a_4 = 1$. His conclusions are that the DE $K_L \rightarrow \pi^+\pi^-\gamma$ branching ratio excludes a small value for the ρ parameter. Ko and Truong [46] and Picciotto [47] have considered the contributions of the reducible anomalous amplitude (term in F_1) and the *indirect* vector interchange (keeping, however, the whole vector pole structure), but not the leading $\mathcal{O}(p^4)$ amplitude : they assume $a_2 = a_4 = 0$. These authors conclude that only a small breaking of the nonet symmetry in the weak sector is compatible with their analysis ($\rho \simeq 0.8, 0.9$) and therefore, that the π^0 pole dominates the $K_L \rightarrow \gamma\gamma$ amplitude. Moreover their results give a small dependence of the magnetic amplitude in the photon energy and, consequently, a too small slope c .

All these previous analyses emphasize that only our Region II is allowed. In our more complete analysis we show that this is not the case and both solutions are kept open. In fact several features (the sign of the slope in $K_L \rightarrow \gamma\gamma^*$ and the ratio f) lead to the scenario described by the parameters in Region I.

A comment about the convergence of the chiral expansion is also interesting. The bulk of the contribution to the width of $K_L \rightarrow \pi^+\pi^-\gamma$ comes from local contributions at $\mathcal{O}(p^4)$ and $\mathcal{O}(p^6)$, but the loop amplitudes are relevant for the region $1.0 < a_2 + 2a_4 \leq 1.4$. The slope in E_γ^* starts at $\mathcal{O}(p^6)$ in χ PT and it is mostly due to the vector exchange but the loop contribution can be as big as 30% and in any case is crucial to give a steady prediction. Local $\mathcal{O}(p^6)$ corrections due to resonance exchange (other than vectors), even if suppressed by heavier masses, could give a non-negligible contribution to the width if numerical factors overcome the suppression. The analysis of $\mathcal{O}(p^8)$ is very much cumbersome. It is curious to notice, however, that the $\mathcal{O}(p^8)$ (and higher orders) amplitude specified in Eq. (38) (that we have not included in our analysis) does not seem smaller than the pure $\mathcal{O}(p^6)$ $M_{ind}^{(6)}$ in Eq. (37) because, in principle, $F_1 \sim \mathcal{O}(1)$. If the chiral expansion has to converge one would expect either a cancellation with other $\mathcal{O}(p^8)$ contributions or that the parameters allow a self-suppression. Hence for our preferred values of $a_2 + 2a_4$, $\rho = 0.8$ implies $F_1 \simeq 0.96$ but $\rho = 0.2$ gives $F_1 \simeq -0.07$ that is one order of magnitude smaller. This fact together with the statement pointed out above that in Region II the $\mathcal{O}(p^6)$ loop corrections to the width are huge indicates that a better convergence of the chiral expansion (in the terms considered here) seems to be achieved with $a_2 + 2a_4$ and ρ small.

6 Conclusion

The measured energy dependence of the spectrum for the process $K_L \rightarrow \pi^+\pi^-\gamma$ shows that the slope of the magnetic amplitude defined in Eq. (32) has a relative big size thought to be due to a relevant vector meson exchange contribution at $\mathcal{O}(p^6)$ in χ PT. Moreover with our present knowledge of the phenomenology the width of the process cannot be predicted in a model independent way. In Ref. [14] we pointed out that the sign of the $K_L \rightarrow \gamma\gamma$ amplitude has to be opposite to the one predicted by pion pole dominance in this decay. Both processes are correlated because receive a reducible contribution depending on the unknown ρ parameter (Eq. (17)) that measures the breaking of the nonet symmetry in the $\mathcal{O}(p^2)$ weak vertex.

In this work we have presented a systematic study of the magnetic amplitude of the process $K_L \rightarrow \pi^+\pi^-\gamma$ up to $\mathcal{O}(p^6)$ in χ PT. We have computed the local contributions (due to a reducible anomalous amplitude and vector meson exchange) and the one-loop magnetic amplitude at this order.

The $\mathcal{O}(p^4)$ magnetic amplitude ($M^{(4)}$) and part of the loop contribution ($M_{N_i}^{(6)}$) are model dependent because the couplings N_i in $\mathcal{L}_4^{|\Delta S|=1}$ Eq. (18) are not known from the phenomenology. We have included the spin-1 resonance exchange contribution to the relevant N_i couplings that we have evaluated in the approach described in Ref. [26]. Moreover part of the vector exchange amplitudes due to diagrams in Fig. 4 where a weak $VP\gamma$ or VPP appear are also not known. Driven by the good description we have achieved in Ref. [14] for the processes $K \rightarrow \pi\gamma\gamma$ and $K_L \rightarrow \gamma\ell^+\ell^-$ we have used the Factorization Model in the Vector Couplings (FMV) [14, 26] in order to provide the *direct* weak $VP\gamma$ and VPP vertices.

The conclusions of our analysis can be stated as follows :

- 1/ We are able to accommodate the experimentally determined branching ratio $Br(K_L \rightarrow \pi^+\pi^-\gamma ; E_\gamma^* > 20 \text{ MeV})_{DE}$ inside a reasonable range of variation of the parameters $a_2 + 2a_4$ and ρ . When combined with the $K_L \rightarrow \gamma\gamma$ amplitude we find two regions for the combination $a_2 + 2a_4$: $0.4 \leq a_2 + 2a_4 \leq 0.8$ and $1.0 < a_2 + 2a_4 \leq 1.4$. Away of this range $|A_{\gamma\gamma}|$ is predicted to differ for more than a factor two of the experimental figure. Remarkably in any of these cases the value given by Eq. (57) is $\eta \leq 0.3$ implying, therefore, that the octet operators are not enhanced and are consistent with the perturbative expectation provided by the Wilson coefficient ($\eta \simeq 0.2$). This we can interpret as a fiducial behaviour of factorization showing that the dynamical features introduced in our analysis through this hypothesis are compatible with the perturbative expansion that becomes predictive at this point.

We have also concluded that the Region II is perhaps sensitive to effects not included here like $\mathcal{O}(p^6)$ axial-vector exchange or non-resonant contributions and $\mathcal{O}(p^8)$ corrections.

- 2/ Independently of the parameter variation we consistently predict a small range for the slope of $K_L \rightarrow \pi^+\pi^-\gamma$, roughly $c \simeq -1.6, -1.8$ in very good agreement with the experimental result $c_{exp} = -1.7 \pm 0.5$. The loop contributions are shown to be crucial to stabilize the slope in this small range. As a consequence the spectrum plotted in Fig. 7 is a pure prediction of our framework. Corrections to it can come from other resonance interchange at $\mathcal{O}(p^6)$ (axial-vectors, scalars, ...) or $\mathcal{O}(p^8)$ effects.
- 3/ From Table 2 we see that, in our joint analysis, both signs of the $K_L \rightarrow \gamma\gamma$ amplitude are consistent with the phenomenology, in contradistinction to the conclusion reached by previous studies. Hence the result $F_2 < 0$ (pion pole dominance implies $F_2 > 0$) is allowed in consistency with our statement in Ref. [14] that the slope in $K_L \rightarrow \gamma\gamma^*$, experimentally determined, would imply that sign. If this is the case we would conclude that, in opposition to previous results [45, 46, 47], a bigger breaking of the nonet symmetry in the weak vertex is called for ($\rho \simeq 0.2$). Of course, at this point, it cannot be excluded a solution with $\rho \simeq 0.8$, and blame the change of sign of the $K_L \rightarrow \gamma\gamma$ amplitude to a, still unknown, huge higher order correction.

The relevance of other resonance exchange generated $\mathcal{O}(p^6)$ or higher order contributions would be very much clarified once a more accurate measurement of the spectrum in E_γ^* is carried out. The experiment KLOE at DAΦNE expects to have 35,000 $K_L \rightarrow \pi^+\pi^-\gamma$ events p/year due to DE with $E_\gamma^* > 20$ MeV [4] and therefore should be able to improve statistics and accuracy in this channel. Other two new experiments NA48 at CERN and KTEV at Fermilab could also bring new features on this process. These are going to focus on the related $K_L \rightarrow \pi^+\pi^-\gamma^*$ process where to keep under theoretical control the leading real photon channel is crucial to disentangle its q^2 dependence.

Acknowledgements

The authors wish to thank F.J. Botella, F. Cornet, G. Ecker, G. Isidori, H. Neufeld and A. Pich for interesting and fruitful discussions on the topics of this paper. J.P. is partially supported by Grant PB94-0080 of DGICYT (Spain) and Grant AEN-96/1718 of CICYT (Spain).

Appendix A : Kinematics on $K_L \rightarrow \pi^+ \pi^- \gamma$

In Section 3 we defined the amplitudes and wrote explicitly the differential cross section for an unpolarized photon in $K_L \rightarrow \pi^+ \pi^- \gamma$. Here, for completeness, we collect some useful kinematical relations [8, 33].

In $K_L \rightarrow \pi^+ \pi^- \gamma$ the most useful variables are : i) the photon energy in the kaon rest frame (E_γ^*), ii) the angle (θ) between the γ and π^+ momenta in the di-pion rest frame. The relations between (E_γ^*, θ) and the z_i defined in Eq. (28) are

$$z_\pm = \frac{E_\gamma^*}{2m_K} (1 \mp \beta \cos \theta), \quad z_3 = \frac{E_\gamma^*}{m_K}, \quad (\text{A.1})$$

where $\beta = \sqrt{1 - 4m_\pi^2/(m_K^2 - 2m_K E_\gamma^*)}$. The kinematical limits on E_γ^* and θ are given by

$$0 \leq E_\gamma^* \leq \frac{m_K^2 - 4m_\pi^2}{2m_K}, \quad -1 \leq \cos \theta \leq 1. \quad (\text{A.2})$$

The differential rate in terms of these variables for an unpolarized photon is

$$\frac{\partial^2 \Gamma}{\partial E_\gamma^* \partial \cos \theta} = \frac{(E_\gamma^*)^3 \beta^3}{512 \pi^3 m_K^3} \left(1 - \frac{2E_\gamma^*}{m_K}\right) \sin^2 \theta (|E|^2 + |M|^2). \quad (\text{A.3})$$

Appendix B : The weak VPP vertex in the Factorization Model in the Vector couplings

Following the same procedure that we used in Ref. [14] to construct the weak $VP\gamma$ vertex we proceed to evaluate the weak VPP vertex for $K_L \rightarrow \pi^+ \pi^- \gamma$.

The bosonization of the Q_- operator in Eq. (20) can be carried out in the FMV from the strong effective action S of a chiral gauge theory. For later use let us split the strong action and the left-handed current into two pieces : $S = S_1 + S_2$ and $\mathcal{J}_\mu = \mathcal{J}_\mu^1 + \mathcal{J}_\mu^2$, respectively. Then in the factorization approach the Q_- operator is represented by

$$Q_- \leftrightarrow 4 \left[\langle \lambda \{ \mathcal{J}_\mu^1, \mathcal{J}_\mu^2 \} \rangle - \langle \lambda \mathcal{J}_\mu^1 \rangle \langle \mathcal{J}_\mu^2 \rangle - \langle \lambda \mathcal{J}_\mu^2 \rangle \langle \mathcal{J}_\mu^1 \rangle \right], \quad (\text{B.1})$$

with $\lambda \equiv (\lambda_6 - i\lambda_7)/2$ and, for generality, the currents have been supposed to have non-zero trace.

In order to apply this procedure to construct the factorizable contribution to the weak $\mathcal{O}(p^3)$ VPP vertex we have to identify in the full strong action the pieces (at this chiral order) that can contribute. It turns out that there are four terms in the strong action that can play a rôle. Analogously to the specified procedure we define correspondingly :

$$\begin{aligned} S &= S_V + S_P, \\ S_V &= S_{V\gamma} + S_{VPP}, \\ S_P &= S_2^X + S_4^X, \end{aligned} \quad (\text{B.2})$$

where the notation is self-explicative and the actions correspond to the lagrangian densities proportional to f_V and g_V in \mathcal{L}_V Eq. (10), \mathcal{L}_2 in Eq. (3) and \mathcal{L}_4 in Eq. (5).

Evaluating the left-handed currents and keeping only the terms of interest we get

$$\begin{aligned}\frac{\delta S_V}{\delta \ell^\mu} &= \frac{f_V}{\sqrt{2}} \left[\partial^\alpha u^\dagger V_{\alpha\mu} u + u^\dagger V_{\alpha\mu} \partial^\alpha u \right] + i \frac{g_V}{\sqrt{2}} u^\dagger [V_{\alpha\mu}, u^\alpha] u, \\ \frac{\delta S_P}{\delta \ell^\mu} &= -\frac{F_\pi^2}{2} u^\dagger u_\mu u + i L_9 \partial^\alpha \left(u^\dagger [u_\alpha, u_\mu] u \right).\end{aligned}\tag{B.3}$$

Then the effective action in the factorizable approach is

$$\begin{aligned}\mathcal{L}_W^{fact}(VPP) &= 4 G_8 \eta_{VPP} \left[\langle \lambda \left\{ \frac{\delta S_V}{\delta \ell^\mu}, \frac{\delta S_P}{\delta \ell_\mu} \right\} \rangle - \langle \lambda \frac{\delta S_V}{\delta \ell^\mu} \rangle \langle \frac{\delta S_P}{\delta \ell_\mu} \rangle \right. \\ &\quad \left. - \langle \lambda \frac{\delta S_P}{\delta \ell^\mu} \rangle \langle \frac{\delta S_V}{\delta \ell_\mu} \rangle \right] + h.c. .\end{aligned}\tag{B.4}$$

There is however an extra contribution that remains to be taken into account. In Ref. [26] we have shown that in the conventional vector formulation one can construct a weak $\mathcal{O}(p)$ coupling involving vectors as

$$\mathcal{L}_{\mathcal{O}(p)}^V = G_8 F_\pi^4 \left[\omega_1^V \langle \Delta \{V_\mu, u^\mu\} \rangle + \omega_2^V \langle \Delta u_\mu \rangle \langle V^\mu \rangle \right],\tag{B.5}$$

where the couplings ω_i^V are in the FM

$$\omega_1^V = \sqrt{2} \frac{m_V^2}{F_\pi^2} f_V \eta_V, \quad \omega_2^V = -\omega_1^V,\tag{B.6}$$

with η_V the unknown factorization factor. If one rotates away these terms through the shift

$$V_\mu \rightarrow V_\mu - \frac{G_8 F_\pi^4}{m_V^2} \left[\omega_1^V \{ \Delta, u_\mu \} + \omega_2^V \langle \Delta u_\mu \rangle \right],\tag{B.7}$$

the kinetic term of the vector mesons

$$\mathcal{L}_K = -\frac{1}{4} \langle V_{\mu\nu} V^{\mu\nu} \rangle + \frac{m_V^2}{2} \langle V_\mu V^\mu \rangle,\tag{B.8}$$

generates also an $\mathcal{O}(p^3)$ weak VPP coupling. In Eq. (B.8) $V_{\mu\nu}$ has been defined in connection with Eq. (10).

Comparing the full lagrangian density $\mathcal{L}_W(VPP)$ in Eqs. (42,43,44) we find the predictions of the FMV model for the couplings σ_i . Using $f_V = 2g_V$ we get

$$\begin{aligned}\sigma_1^{FMV} &= \frac{f_V}{\sqrt{2}} \left[\eta_V + 4 L_9 \frac{m_V^2}{F_\pi^2} \eta_{VPP} \right], \\ \sigma_2^{FMV} &= -\sqrt{2} f_V \eta_V, \\ \sigma_3^{FMV} &= -\sqrt{2} f_V \left[\eta_V + 2 L_9 \frac{m_V^2}{F_\pi^2} \eta_{VPP} \right].\end{aligned}\tag{B.9}$$

Appendix C : Loop integrals

Here we collect the functions appearing in the loop contributions to the magnetic amplitude.

The function $K[q^2, m_i^2, m_j^2]$ appearing in the loop contributions to the magnetic amplitude $M_{WZW}^{(6)}$ Eq. (51) and $M_{N_i}^{(6)}$ Eq. (52) is defined through

$$\int \frac{d^4\ell}{(2\pi)^4} \frac{\ell^\mu \ell^\nu}{[\ell^2 - m_i^2][(\ell - q)^2 - m_j^2]} = i g^{\mu\nu} q^2 B_{22}[q^2, m_i^2, m_j^2] + \dots, \quad (\text{C.1})$$

as

$$q^2 B_{22}[q^2, m_i^2, m_j^2] |_{\overline{MS}} = \left(\frac{m_K}{4\pi}\right)^2 K[q^2, m_i^2, m_j^2], \quad (\text{C.2})$$

where in the \overline{MS} scheme the term proportional to $\lambda_\infty = \frac{2}{D-4} - (\Gamma'(1) + \ln(4\pi) + 1)$ appearing in $B_{22}[q^2, m_i^2, m_j^2]$ has been subtracted.

The $F[q^2, m^2]$ function defined in the same loop amplitudes is

$$F[q^2, m^2] = \left(1 - \frac{x}{4}\right) \sqrt{1 - \frac{4}{x}} \ln\left(\frac{\sqrt{x-4} + \sqrt{x}}{\sqrt{x-4} - \sqrt{x}}\right) - 2, \quad (\text{C.3})$$

with $x = q^2/m^2$ (note that this function is usually quoted in the literature [37] with an extra factor of m^2).

For equal masses the K and F functions are related as

$$K[q^2, m^2, m^2] = -\frac{1}{12m_K^2} \left[(6m^2 - q^2) \ln\left(\frac{m^2}{\mu^2}\right) + \frac{5}{3}q^2 + 4F[q^2, m^2] \right]. \quad (\text{C.4})$$

References

- [1] S. Weinberg, *Physica*, **96A** (1979) 327.
- [2] J. Gasser and H. Leutwyler, *Ann. of Phys.*, **158** (1984) 142;
J. Gasser and H. Leutwyler, *Nucl. Phys.*, **B250** (1985) 465.
- [3] J.L. Ritchie and S.G. Wojcicki, *Rev. Mod. Phys.*, **65** (1993) 1149;
L. Littenberg and G. Valencia, *Ann. Rev. Nucl. Part. Sci.*, **43** (1993) 729;
B. Winstein and L. Wolfenstein, *Rev. Mod. Phys.*, **65** (1993) 1113;
G. D'Ambrosio and G. Isidori, "CP violation in Kaon decays", Preprint INFNNA-IV-96/29, LNF-96/033(P), to be published in *Int. J. of Mod. Phys. A*; hep-ph/9611284.
- [4] G. D'Ambrosio, G. Ecker, G. Isidori and H. Neufeld, "Radiative non-leptonic kaon decays" in "The Second DAΦNE Physics Handbook", ed. by L. Maiani, G. Pancheri and N. Paver, LNF (1995), p. 265.
- [5] G. Ecker, H. Neufeld and A. Pich, *Phys. Lett.*, **B278** (1992) 337.
- [6] J. Bijnens, G. Ecker and A. Pich, *Phys. Lett.*, **B286** (1992) 341.
- [7] G. Ecker, H. Neufeld and A. Pich, *Nucl. Phys.*, **B413** (1994) 321.
- [8] G. D'Ambrosio and G. Isidori, *Z. Phys.*, **C65** (1995) 649.
- [9] G. Ecker, J. Gasser, A. Pich and E. de Rafael, *Nucl. Phys.*, **B321** (1989) 311.
- [10] J.F. Donoghue, C. Ramirez and G. Valencia, *Phys. Rev.*, **D39** (1989) 1947.
- [11] A. Pich and E. de Rafael, *Nucl. Phys.*, **B358** (1991) 311.
- [12] G. Ecker, J. Kambor and D. Wyler, *Nucl. Phys.*, **B394** (1993) 101.
- [13] C. Bruno and J. Prades, *Z. Phys.*, **C57** (1993) 585.
- [14] G. D'Ambrosio and J. Portolés, *Nucl. Phys.*, **B492** (1997) 417.
- [15] Yu. P. Malakian, *Sov. J. Nucl. Phys.*, **26** (1977) 337; *Nucl. Phys.*, **B133** (1978) 145;
J.L. Lucio, *Phys. Rev.*, **D24** (1981) 2457.
See also
M. McGuigan and A.I. Sanda, *Phys. Rev.*, **D36** (1987) 1413.
- [16] A.V. Manohar and H. Georgi, *Nucl. Phys.*, **B234** (1984) 189.
- [17] J. Wess and B. Zumino, *Phys. Lett.*, **B37** (1971) 95;
E. Witten, *Nucl. Phys.*, **B223** (1983) 422.

- [18] S. Coleman, J. Wess and B. Zumino, *Phys. Rev.*, **177** (1969) 2239;
C.G. Callan, S. Coleman, J. Wess and B. Zumino, *Phys. Rev.*, **177** (1969) 2247.
- [19] G. Ecker, J. Gasser, H. Leutwyler, A. Pich and E. de Rafael, *Phys. Lett.*, **B223** (1989) 425.
- [20] Review of Particle Properties, R.M. Barnett et al., *Phys. Rev.*, **D54** (1996) 1.
- [21] G. Ecker, A. Pich and E. de Rafael, *Phys. Lett.*, **B237** (1990) 481.
- [22] M. Bando, T. Kugo and K. Yamawaki, *Phys. Rep.*, **164** (1988) 217;
T. Fujikawa, T. Kugo, H. Terao, S. Uehara and K. Yamawaki, *Progr. of Theor. Phys.*, **73** (1985) 926.
- [23] J. Prades, *Z. Phys.*, **C63** (1994) 491.
- [24] M.C. Birse, *Z. Phys.*, **A355** (1996) 231.
- [25] E. Pallante and R. Petronzio, *Nucl. Phys.*, **B396** (1993) 205.
- [26] G. D’Ambrosio and J. Portolés, “Spin-1 resonance contributions to the weak Chiral Lagrangian: the vector formulation”, Preprint INFNNA-IV-97/27, DSFNA-IV-97/27, (1997).
- [27] J.F. Donoghue, E. Golowich and B.R. Holstein, “Dynamics of the Standard Model”, (Cambridge University Press, 1992);
G. Ecker, *Prog. Part. Nucl. Phys.*, **35** (1995) 1;
A. Pich, *Rept. Prog. Phys.*, **58** (1995) 563.
- [28] M.K. Gaillard and B.W. Lee, *Phys. Rev. Lett.*, **33** (1974) 108;
G. Altarelli and L. Maiani, *Phys. Lett.*, **B52** (1974) 351;
M.A. Shifman, A.I. Vainshtein and V.I. Zakharov, *Nucl. Phys.*, **B120** (1977) 316;
F.J. Gilman and M.B. Wise, *Phys. Rev.*, **D20** (1979) 1216;
M. Ciuchini, E. Franco, G. Martinelli and L. Reina, “Estimates of ε'/ε ” in “The Second DAΦNE Physics Handbook”, Ed. by L. Maiani, G. Pancheri and N. Paver, LNF (1995), p. 27;
G. Buchalla, A.J. Buras and M.E. Lautenbacher, *Rev. Mod. Phys.*, **68** (1996) 1125.
- [29] J. Kambor, J. Missimer and D. Wyler, *Nucl. Phys.*, **B346** (1990) 17.
- [30] G. Esposito–Farèse, *Z. Phys.*, **C50** (1991) 255.
- [31] H.-Y. Cheng, *Phys. Rev.*, **D42** (1990) 72.
- [32] F.E. Low, *Phys. Rev.*, **110** (1958) 974.

- [33] G. D’Ambrosio, M. Miragliuolo and P. Santorelli, “Radiative non-leptonic kaon decays” in “The DAΦNE Physics Handbook”, Eds. L. Maiani, G. Pancheri and N. Paver, LNF (1992) p. 231.
- [34] Y.-C.R. Lin and G. Valencia, *Phys. Rev.*, **D37** (1988) 143.
- [35] E.J. Ramberg et al., *Phys. Rev. Lett.*, **70** (1993) 2525.
- [36] P. Heiliger and L.M. Sehgal, *Phys. Rev.*, **D47** (1993) 4920.
- [37] J. Bijnens, A. Bramon and F. Cornet, *Phys. Lett.*, **B237** (1990) 488.
- [38] R. Akhoury and A. Alfakih, *Ann. of Phys.*, **210** (1991) 81.
- [39] M.K. Gaillard and B.W. Lee, *Phys. Rev.*, **D10** (1974) 897;
 E. Ma and A. Pramudita, *Phys. Rev.*, **D24** (1981) 2476;
 G. D’Ambrosio and D. Espriu, *Phys. Lett.*, **B175** (1986) 237;
 J. L. Goity, *Z. Phys.*, **C34** (1987) 341;
 L.L. Chau and H.-Y Cheng, *Phys. Rev. Lett.*, **54** (1985) 1768; *Phys. Lett.*, **B195** (1987) 275 ;
 F. Buccella, G. D’Ambrosio and M. Miragliuolo, *Nuovo Cimento*, **104A** (1991) 777.
- [40] J.F. Donoghue, B.R. Holstein and Y.-C.R. Lin, *Nucl. Phys.*, **B277** (1986) 651.
- [41] J.L. Goity and L. Zhang, *Phys. Lett.*, **B398** (1997) 387.
- [42] N.A. Roe et al., *Phys. Rev.*, **D41** (1990) 17.
- [43] E.P. Venugopal and B.R. Holstein, “*Chiral anomaly and η - η' mixing*”; hep-ph/9710382.
- [44] J.F. Donoghue and B.R. Holstein, *Phys. Rev.*, **D29** (1984) 2088.
- [45] H.-Y. Cheng, *Phys. Lett.*, **B245** (1990) 122.
- [46] P. Ko and T.N. Truong, *Phys. Rev.*, **D43** (1991) R4.
- [47] C. Picciotto, *Phys. Rev.*, **D45** (1992) 1569.